



HAL
open science

Supramolecular Approaches to Graphene: From Self-Assembly to Molecule-Assisted Liquid-Phase Exfoliation

Artur Ciesielski, Paolo Samorì

► **To cite this version:**

Artur Ciesielski, Paolo Samorì. Supramolecular Approaches to Graphene: From Self-Assembly to Molecule-Assisted Liquid-Phase Exfoliation. *Advanced Materials*, 2016, 28 (29), pp.6030-6051. 10.1002/adma.201505371 . hal-03631849

HAL Id: hal-03631849

<https://hal.science/hal-03631849>

Submitted on 5 Apr 2022

HAL is a multi-disciplinary open access archive for the deposit and dissemination of scientific research documents, whether they are published or not. The documents may come from teaching and research institutions in France or abroad, or from public or private research centers.

L'archive ouverte pluridisciplinaire **HAL**, est destinée au dépôt et à la diffusion de documents scientifiques de niveau recherche, publiés ou non, émanant des établissements d'enseignement et de recherche français ou étrangers, des laboratoires publics ou privés.

DOI: 10.1002/ ((please add manuscript number))

Article type: Review

Supramolecular approaches to graphene: From self-assembly to molecule assisted liquid-phase exfoliation

Artur Ciesielski and Paolo Samorì**

Dr. A. Ciesielski, Prof. P. Samorì
Nanochemistry Laboratory, ISIS & icFRC, Université de Strasbourg & CNRS,
8 allée Gaspard Monge, 67000 Strasbourg, France
E-mail: samori@unistra.fr , ciesielski@unistra.fr

Keywords: graphene, non-covalent functionalization, liquid-phase exfoliation, supramolecular chemistry

Abstract

Graphene, a one-atom thick two-dimensional (2D) material, is at the core of an ever-growing research effort due to its combination of unique mechanical, thermal, optical and electrical properties. Two strategies are being pursued for the graphene production: the *bottom-up* and the *top-down*. The former relies on the use of covalent chemistry approaches on properly designed molecular building blocks undergoing chemical reaction to form 2D covalent networks. The latter occurs *via* exfoliation of bulk graphite into individual graphene sheets. Amongst the various types of exfoliations exploited so far, ultrasound-induced liquid-phase exfoliation (UILPE) is an attractive strategy, being extremely versatile, up-scalable and applicable to a variety of environments. In this review, we highlight the recent developments that have led to successful non-covalent functionalization of graphene and how the latter can be exploited to promote the process of molecule-assisted UILPE of graphite. The functionalization of graphene with non-covalently interacting molecules, both in dispersions as well as in dry films, represents a promising and modular approach to tune various physical and chemical properties of graphene, eventually conferring to such a 2D system a multifunctional nature.

1. Introduction

Graphene has emerged in the last decade as an exciting material possessing unique mechanical, optical, thermal and electrical properties.^[1] Because of this reason it holds potential to impact future emerging technologies, including flexible and wearable electronics.^[2] Numerous other technological applications of graphene are being extensively explored,^[3] including solar cells,^[4, 5] light-emitting devices,^[6] photodetectors,^[7, 8, 9, 10] touch screens,^[11] spin valves,^[12, 13] ultrafast lasers,^[14, 15] and biological labelling^[16] to name a few. Furthermore, its surface area, experimentally measured being as high as $700 \text{ m}^2 \text{ g}^{-1}$,^[17, 18] have made graphene an appealing component for applications in energy^[17, 19, 20, 21] and gas^[22, 23, 24] storage, energy conversion,^[17, 25] micro- and optoelectronics,^[26, 27, 28, 29] as well as in and catalysis.^[30, 31] Nevertheless, the translation of these outstanding properties, which are observed on lab-scale experiments, into real-world applications on an industrial scale suffers from major drawbacks associated to graphene production.

Two approaches are being undertaken to produce graphene, i.e. *bottom-up* and *top-down*.^[32, 33] The former includes the production of graphene's very high quality sheets yet in limited quantities by exploiting the covalent assembly of suitably designed small molecular building blocks, undergoing chemical reaction to generate 2D covalent networks. Unfortunately, *bottom-up* techniques, and in especially those based on organic syntheses starting from small molecular modules,^[34, 35, 36] when performed in liquid media, are both size limited, because macromolecules become less soluble with the increasing size,^[35] and suffer from the occurrence of side reactions with the increasing molecular weight.^[35] The growth on (catalytically active) solid surfaces makes it possible to circumvent these issues. Substrate-based growth can also be achieved by chemical vapour deposition (CVD),^[37, 38] or *via* silicon evaporation from silicon carbide,^[39] which rely on the ability to follow a narrow thermodynamic path. Though the wafer-scale synthesis of graphene has been effectively carried out recently,^[40] this mass-produced material frequently exhibits more modest

properties when compared to pristine graphene isolated by exploiting the ‘scotch tape approach’. *Top-down* approaches, which rely on the exfoliation of the three-dimensional graphite into the two-dimensional graphene, can be accomplished under different environmental conditions.^[41, 42] While defect-free sheets can be obtained by exploiting the micromechanical cleavage,^[43] approaches such as ball-milling^[44, 45, 46, 47, 48, 49] can trigger the formation of defects in graphene. Amongst the *top-down* approaches, liquid-phase exfoliation (LPE), which can be further sub-divided into different methods, i.e. solvothermal-assisted LPE (SALPE),^[50, 51] electrochemical LPE (ELPE),^[52, 53, 54, 55, 56] high-shear mixing (HSM),^[57, 58] ultrasound-induced LPE (UILPE),^[59, 60, 61, 62, 63, 64, 65] and the use of superacids,^[66] represents an extremely versatile approach which can be carried out in a variety of environments. While *bottom-up* methods, and in particular CVD, can yield large size, LPE gives limited sheet sizes.^[61, 67, 68, 69] Nevertheless, LPE has several advantages. It is a viable cost effective process, which can be easily up-scaled to mass-produced dispersions. These inks can be processed on surfaces and interfaces by making use of well-established techniques, such as spin-coating, drop-casting, screen-printing, ink-jet printing and potentially also roll-to-roll (R2R).^[70, 71, 72] High-yield exfoliation and dispersion of graphene in high quantities into the liquid phase is crucial for fundamental studies as well as for practical applications.^[2] Although the aggressive oxidation of graphite, pioneered by Brodie,^[73] Staudenmaier,^[74] and Hummers,^[75] allows its exfoliation in polar solvents, it results in a major re-hybridization of the sp^2 carbons of the pristine graphene into sp^3 , thereby altering drastically the exceptional physical properties of the material.^[76] The oxides that are formed, i.e. carboxyl and hydroxyl groups as well as the epoxy bridges, can be (partially) removed by reduction of the GO to form rGO. Such a reduction can be carried out using chemical, electrochemical and thermal processes. However, as in all cases the reduction process does not allow to reduce the GO with a yield $> 95\%$, many structural defects are still present in rGO. Because of this reason, the physical properties of the rGO^[77, 78, 79, 80] are markedly different from those of the pristine

graphene. Among the various altered characteristics, the disruption of the band structure of graphene upon oxidation reduces its high electrical and thermal conductivity that make graphene exceptional. Nevertheless, in some applications the use of GO and rGO can be beneficial as they feature great chemical complexity. In addition to being component in electronic devices,^[81, 82] GO and rGO have been successfully used in catalysis,^[83, 84] energy storage,^[85] and biomedical applications.^[86]

The characteristic graphene band structure leads to an extraordinary high electron mobility thus allowing graphene-based transistors to process data at very high rates. On the other hand, the lack of band gap makes it difficult to turn off the flowing current. This hinders the implementation of graphene in (nano)electronics. Therefore, it is crucial to open a band gap in graphene to confer to this material a semiconducting nature to also precisely control the charge carrier type (*p*-type vs. *n*-type) and density.

Another major challenge when dealing with graphene, and more generally with carbon allotropes, is its controlled processing.^[87] Hitherto graphene has been found to be processable only in a very few solvents; however, re-aggregation into graphitic material occurs even in these special solvents. Such a re-aggregation can be hindered by combining graphene with suitably designed molecules. The interaction between these two “nano-objects” can be modulated by exploiting a supramolecular approach, the latter relying on the non-covalent functionalization of graphene with small molecular building blocks. Such interaction tailoring can offer substantial advantages in terms of processing of graphene and tunability of the properties of this wonder 2D material, thereby opening novel pathways in various research fields.

The functionalization of graphene with molecules interacting at the non-covalent level, both in dry films as well as in dispersions, has recently gathered a great interest, and the fundamental knowledge of this process has increased substantially. In this review, we discuss the principles of the supramolecular approach applied to graphene, which led to the successful

modification of graphene properties and enhancement in its production in liquid media. In particular, we discuss the use of molecular self-assembly as a method towards the non-covalent functionalization of graphene. We then describe the UILPE of graphite and methods that are employed for the characterization of graphene produced thereof. We also highlight a variety of successful UILPE results by categorizing them into two major classes, i.e. molecule-free and molecule-assisted UILPE.

2. When graphene meets molecules – the supramolecular approach

The interaction between graphene and molecules is accompanied by an adjustment of the properties of both initial components. Such interaction can occur *via* the physisorption of molecular building blocks through non-covalent interactions or through the chemisorption of reactive species undergoing chemical reactions with graphene to form covalent bonds onto its basal plane. Numerous approaches have been devised to tailor the electronic properties of graphene. In particular, atomic chemical doping by nitrogen or boron atoms has been proposed as a way to open the band gap and form *p*-type or *n*-type graphene.^[88, 89] Nevertheless, the doping is typically difficult to be controlled and frequently introduces defects and thus destroys the band structure. Another approach relies on the covalent modification, where the chemisorbed molecules form chemical bonds with graphene.^[90, 91, 92] However, since the covalent bond formation occurs through sp^2 to sp^3 hybridization, it often leads to undesirable modification or even destruction of the graphene electronic properties. Alternatively, the electronic properties of graphene can be modified by non-covalent functionalization,^[93, 94, 95, 96] where the interactions between graphene and adsorbates are dispersive. Following such a strategy the properties that make unique graphene are retained. It is well known that aliphatic or aromatic molecules can adsorb on sp^2 carbon-based surfaces, forming highly ordered supramolecular (crystalline) architectures. Consequently, this approach is very useful to create a periodic electronic modulation of the graphene surface *via*

self-assembly. Generally, molecular self-assembly from solution at surfaces and interfaces towards the formation of an ordered 2D structure takes place under thermodynamically control, being governed by the subtle balance between molecule–substrate, molecule–molecule, solvent–substrate and molecule–solvent interactions.

Van der Waals forces play a major role in the process of adsorption of atoms and molecules on the basal plane of the atomically flat surface of graphene. Van der Waals interactions originate from London dispersion forces,^[97, 98] which emerge from the attraction between the instantaneous dipoles generated by atomic electron clouds. London dispersion forces can be exploited to stabilize the 2D non-covalent architectures, and in particular by functionalizing the molecules with long aliphatic substituents. The formation of crystalline patterns is triggered by the interdigitation of alkyl chains belonging to adjacent molecules.^[99] This process takes place *via* entangling of an alkyl chain in-between two neighboring ones with an energy of interaction of ca. 0.7 kcal mol⁻¹ per methylene unit,^[100] which is ca. four times lower than the energy of adsorption of methylene unit on graphene.^[101] In the case of (poly)aromatic molecules π - π interactions govern the molecular assembly, and therefore these molecules have a strong tendency to stack over each other and over graphene. In particular, the computed values of π - π interaction energy of benzene with graphite/graphene may fluctuate between 8.6 to 11.1 kcal mol⁻¹ for common density functional theory (DFT) and force field calculations,^[102] as compared to the experimental values of 11.5 kcal mol⁻¹ determined from thermal desorption experiments.^[103] Noteworthy, in molecules constituted by the same number of carbon atoms, the interactions between alkanes and graphene are stronger than the ones between poly-aromatics and graphene. This effect that can be explained in terms of the larger polarizability of hydrogen atoms relative to carbon, which is expected to enhance the interaction with graphene surface. The desorption barrier of hexane from graphite has been indeed estimated as 17 kcal mol⁻¹.^[101] In analogy to large aromatic compounds,^[104] these superficial large exothermic deviations are strongly countered by endothermic de-solvation

phenomena. The exothermic nature of the adsorption process can be heavily influenced by the choice of the solvent.

By and large, in the case of aliphatic and aromatic molecules the molecular assembly is governed by van der Waals and π - π interactions, respectively, and regardless of the type of the non-covalent forces these molecules have a strong tendency to interact with graphene, which will certainly make it appealing for future applications in (nano)electronics. Section 3 of this review will highlight the advances of this approach.

For a number of years before the ‘graphene rush’ had started, various groups had investigated the exfoliation and dispersion of carbon nanotubes (CNTs) in solvents.^[67] In 2008, by combining experimental results with thermodynamic modeling Coleman and co-workers demonstrated that the best solvents for the CNTs exfoliation possess surface energies similar to that of the nanotubes.^[105] Once the role of surface energy was established, it became immediately clear that because graphite has a surface energy similar to that of carbon nanotubes, it might be possible to exfoliate graphite into graphene using the very same solvents. A successful exfoliation of graphite towards graphene requires the overcoming of the van der Waals attractions between the adjacent sheets. One among the most effective and straightforward approaches to reduce the strength of the van der Waals interactions is the liquid immersion, where the potential energy between adjacent graphene sheets is given by the dispersive London interactions, which in the presence of a liquid media are considerably reduced with respect to vacuum. The distance between adjacent sheets of graphene in pristine graphite amounts to 3.35 Å. While the van der Waals interactions among adjacent sheets are weak enough to let them slide over each other in the direction perpendicular to the *c*-axis, the attraction is strong enough to inhibit the exfoliation of graphite into individual graphene sheets. This issue can be overcome by applying external physical forces to the graphite immersed in the solvent thereby promoting the graphite exfoliation. Among different physical forces the use of ultrasound in liquid environments is a viable method to extract individual

layers.^[14, 61, 63, 67, 68, 106, 107, 108, 109] During UILPE the exfoliation of graphite occurs thanks to the shear forces and the cavitation, acting on the bulk material during ultrasonication. Acoustic waves, in fact, consist of alternating regions of compression and rarefaction transmitting in a medium along the wave propagation direction. When a negative pressure is exerted onto a liquid, the van der Waals interactions between the molecules are overcome and micrometer size bubbles of gas or cavities are grown, nucleate and then collapse.^[110] This phenomenon is known as cavitation. When the bubbles collapse against graphite, this determines a shockwave resulting in the fragmentation of the graphite. On the other hand, when the bubbles collapse in the liquid in the proximity of the graphite flakes, a jet of liquid hits the graphite. Following the theory of stress waves, once a compressive wave enters in contact with the plane of graphite a tensile stress on the graphite has to be reflected back causing the exfoliation (Figure 1). A second phenomenon, which causes the exfoliation, is the unbalanced lateral compressive stress, which will cause a shear effect causing delamination and dispersion of the flakes (Figure 1). Finally, the jet of liquid can also penetrate in-between two graphene sheets causing the separation, i.e. the exfoliation of the individual sheets.^[41, 111] After the exfoliation, the solvent-graphene interaction needs to balance the inter-sheet attractive forces. Interestingly, the use of a molecule such as a surfactant when properly selected can promote the exfoliation of graphite into graphene, even in solvents such as water, where the potential of the surfactant-coated graphene nanosheets controls the dispersed concentration.^[68] Moreover, the use of *ad hoc* molecules can be exploited to enhance the performance of UILPE in organic solvents, in particular when the molecules have a high energy of adsorption on the basal plane of graphene, being higher than the one of the solvent molecules interacting with the graphene. Pioneering contributions towards the quantitative understanding of molecular adsorption on carbonaceous surfaces have come from temperature programmed desorption (TPD), where early analyses of linear alkanes on graphite have shown that the binding energy increases linearly with the number of carbon atoms in the

alkane chain,^[112] with each methylene group contributing $\sim 2 \text{ kcal mol}^{-1}$.^[113] Nevertheless, with longer alkanes it was discovered that the increased configurational entropy loss upon physisorption decreases the total binding energy per carbon atom, which results in a non-linear dependence of the desorption energy on the chain length.^[114] TPD analyses on a range of polycyclic aromatic hydrocarbons (PAHs) provided a lower binding energy per carbon atom of $\sim 1.2 \text{ kcal mol}^{-1}$.^[103] Because the self-assembly of molecules at graphene surface is primarily driven by the thermodynamics, the design of the molecules used during the UILPE processes can be very challenging, and depending of the chosen solvent can require the modification of their chemical structure/nature. In particular, in the case of the charged molecules used in aqueous dispersions, the stabilization of graphene sheets occurs *via* the interplay between molecule-graphene interactions and repulsive forces between surfactant-coated flakes. Slightly different types of interactions have to be considered in the case of organic dispersions, where apolar molecules are used and interact with graphene through van der Waals forces and therefore π - π re-stacking between graphene sheets is thermodynamically hindered. UIPLE and molecule-assisted UILPE will be discussed in details in Section 4.

3. Non-covalent functionalization of graphene

Over the past decade, the self-assembly of molecular building blocks on graphite surface has attracted a considerable attention because it represents a *bottom-up* approach for tailoring interfaces with a sub-nm precision, ultimately producing under thermodynamic control structurally well-defined functional nanostructures through the proper design of organic molecules.^[99, 115, 116, 117, 118] Given that graphite can be seen as a stack of graphene sheets, the knowledge gathered on the formation of supramolecular patterns on graphite can be potentially transferred for the non-covalent functionalization of graphene.^[119, 120] In general, the research on non-covalent functionalization of graphene, i.e. the functionalization of graphene with ordered supramolecular patterns, is targeting two challenges: (i) the

understanding and control over the intermolecular and interfacial interactions in order to decorate surfaces with complex multicomponent ordered assemblies, (ii) the modulation of the physico-chemical properties of graphene for technologically relevant purposes such as doping or facilitating atomic layer deposition.

3.1. Non-covalent functionalization of graphene: towards structural complexity

Early attempts of molecular functionalization of graphene were focused on the characterization and comparison of self-assembled patterns on the basal plane of epitaxial graphene (EG) prepared by CVD, with self-assembled monolayers generated on highly oriented pyrolytic graphite (HOPG).^[121, 122, 123] The need to explore well-ordered patterns at the molecular scale has made Scanning Tunneling Microscopy (STM)^[124, 125] an extensively employed and extremely powerful tool to study supramolecular materials with a sub-molecular resolution.^[126, 127, 128, 129, 130] The sub-nanometer resolution that can be reached by STM makes it possible to gain exhaustive information on the interactions between molecule-molecule and molecule-graphene (or graphite) surface. In the last years, the majority of the investigations of the non-covalent functionalization of graphene were focused on well-known organic semiconductors featuring an extended aromaticity taking advantage of their unique chemical structure promoting π - π interactions with graphene. This includes perylene-3,4,9,10-tetracarboxylic dianhydride (PTCDA), fullerene and metallophthalocyanines (MPc), see Figure 2.

The pioneering work of Lauffer and co-workers in 2008,^[121] showing that PTCDA self-assembled patterns can be grown on graphene bilayers supported on SiC(0001), has been a source of inspiration for several groups.^[122, 123, 131, 132] It has been found that PTCDA molecules self-assemble on graphene in the similar fashion as on HOPG surface, i.e. the molecules adsorb flat on the surface with their aromatic core parallel to the basal plane of graphene. The supramolecular structure is stabilized both by molecule-graphene π - π

interactions and by intermolecular C-H \cdots O-C hydrogen bonds. Typical STM image of PTCDA molecules arranged in a herringbone motif on EG/SiC(0001) is portrayed in Figures 3a-b.

Metallophthalocyanines (MPc) represents another class of aromatic compounds investigated on EG grown on various metal substrates such as Ru(0001), Ni(111), Pt(111) or Ir(111), to name a few.^[133, 134, 135, 136, 137, 138, 139, 140, 141] EG has relatively strong interactions with substrates such as Ru(0001) or Ni(111), whereas it interacts weakly with Ir(111) and SiC(0001).^[142] While graphene grown on weakly interacting substrates exhibits HOPG-like adsorption landscapes, once grown on strongly interacting substrates it displays moiré superlattice, which strongly affects the molecular physisorption. In 2009 Gao and co-workers investigated the self-assembly of various phthalocyanines on an epitaxial graphene monolayer by means of STM.^[133] The formation of regular Kagome lattices (Figure 3c), which duplicates the lattice of the moiré pattern of single layer graphene (SLG), was observed, demonstrating that SLG can act as a template for the fabrication of supramolecular architectures. Moreover, by varying the central metal ion of the phthalocyanine, the molecule self-assemble into Kagome lattices with tunable molecular spins. More recently, Sainio and co-workers investigated the adsorption of CoPc molecules on SLG on Ir(111),^[138] and showed that CoPc self-assembles on SLG at room temperature, forming a nearly square lattice (Figure 3d). In contrast to previous studies of SLG interacting strongly with metallic substrates, and with more strongly corrugated moiré structures, the moiré pattern on Ir(111) does not affect the self-assembled structure of CoPc.

To date, various examples of C₆₀ self-assembly on EG have been reported,^[143, 144, 145, 146] and show that differently than in the case of Pc, the supramolecular architectures formed by C₆₀ molecules are not substrate dependent, and close-packed structures are formed on SLG grown on either strongly or weakly interacting metallic supports (see Figures 3e and 3f).

Behm and co-workers also explored the influence of graphene superlattice on molecular adsorption,^[147] and showed that the influence of moiré corrugation is even more drastic in the case of 2-phenyl-4,6-bis(6-(pyridin-3-yl)-4-(pyridin-3-yl)pyridin-2-yl)-pyrimidine (3,3'-BTP, Figure 2). 3,3'-BTP molecules form supramolecular networks stabilized by weak C-H...N intermolecular hydrogen bonds and π - π molecule/graphene interactions. The physisorption of 3,3'-BTP on EG/Ru(0001) resulted in the formation of multiple random architectures that include triangular, linear and circular structures. This behavior of 3,3'-BTP molecules is in stark contrast to that observed on HOPG, wherein well-ordered 2D patterns were monitored.^[148] On EG/Ru(0001) the molecules exclusively occupied the 'valley' sites while most of the bright 'hill' sites remained vacant. This observation was found being in good accordance with theoretical calculations, which revealed the difference in adsorption energy between 'valley' and 'hill' sites as high as ~ 0.36 eV.

De Feyter and co-workers investigated the molecular self-assembly at the interface between graphene and organic solution.^[149] The formation of supramolecular networks of a dehydrobenzo[12]annulene derivative equipped with long alkoxy chains containing diacetylene units (DBA, Figure 2) was explored on different types of graphene, i.e. EG/SiC(0001), EG/Cu and exfoliated graphene on mica. DBA formed well-ordered 2D porous networks on all three types of graphene. These networks are held together by van der Waals interactions between interdigitated alkoxy chains and between DBAs and graphene.

The field of investigation of molecular assembly on graphene is at its infancy, and there are plenty of opportunities to tailor more and more complex and multicomponent supramolecular structures on graphene surface. Achieving a higher control over the non-covalent functionalization of graphene will be key, as it will make it possible to decorate this unique 2D material with *ad hoc* functional groups in pre-defined positions. Towards this end, beside the extensive use of π - π and van der Waals interactions, two other non-covalent forces featuring greater geometrical control such as H-bonding and metallo-ligand interactions will

be valuable tools to improve the structural and functional complexity of self-assembled monolayers on graphene.

3.2. Non-covalent functionalization of graphene: modulating the physico-chemical properties of graphene for functional applications

Besides the interest in controlling the molecular self-assembly on graphene to unravel how one can modulate the physical properties of graphene, such a supramolecular approach is also appealing for technological perspectives, as it may be used to tune the doping upon physisorption of ordered arrays of organic molecules. In this sub-section we will highlight a few examples on the effect of the supramolecular organization on the electrical properties of graphene. Although there are quite a number of examples on doping graphene with organic molecules, we will focus exclusively on those based on patterns whose order at the supramolecular level has been proven and detailed by the means of structural mapping through STM and/or Atomic Force Microscopy (AFM) imaging.

Recently, De Feyter and co-workers have demonstrated that *cis*-1-amino-9-octadecene, also known as oleylamine (OA, Figure 2), self-assembles into ordered lamellar structures on both HOPG and graphene surfaces.^[150] The detailed molecular ordering was investigated by AFM and STM. The latter tool showed that the OA molecules arrange in a head-to-head non-interdigitated fashion with their carbon chains lying parallel on the basal plane of the surfaces and running perpendicular to the lamellar directions (Figure 4a). To examine the electronic interaction effects of OA pattern in graphene, back-gated graphene field-effect transistor (G-FET) devices (Figure 4b) were characterized electrically. Figure 4c shows the transfer curves of drain current (I_{ds}) vs. back-gate voltage (V_g) for a G-FET device before and after formation of self-assembled OA structures. Interestingly, the doping levels were tuned by varying the OA deposition conditions, with the maximum electron doping concentration up to 7.7×10^{12} cm².

In 2010 Neves and co-workers showed that *p*-type doping of graphene can be achieved under ambient conditions through non-covalent functionalization of graphene with octadecylphosphonic acid (OPA, Figure 2) molecules.^[151] AFM images demonstrated that OPA molecules, which comprise phosphonic acid headgroups on linear alkyl chains (Figure 5a), self-assemble into ordered 2D crystals by drop-casting onto SLG surface (prepared by mechanical exfoliation), supported on SiO₂. Raman spectroscopy analysis of OPA-functionalized graphene revealed that the position of graphene G peak shifts to higher wavelengths. Moreover, the width at half maximum of this peak is significantly reduced compared to pristine graphene (Figure 5b).

Feringa and co-workers used bis-urea substituted ter-thiophene derivative (BUT₃, Figure 2) as a molecular building block for functionalizing CVD graphene.^[152] A combined STM study of the self-assembly of molecular lamellas formed on graphene surface and its effect on the electrical properties of graphene showed that commercially available CVD graphene can be used as a substrate for the self-assembly of BUT₃ molecules into ordered architectures. Changes in charge carrier mobility and in doping levels were observed in G-FET after BUT₃ functionalization.

The possibility of tuning graphene properties by its non-covalent functionalization with highly ordered molecular nanopatterns remains an interesting and versatile method, which will certainly be explored in the upcoming years. Although a body of literature generated to date on organic functionalization of graphene demonstrates its potential, the control and tunability of the electronic properties of graphene remain unexplored. Using the supramolecular chemistry, it will be possible to precisely tune the position and density of functional groups on graphene surface, therefore allowing attaining a full control and ultimately harnessing the doping process. Moreover, in the recent years graphene has emerged as interesting substrate to carry out biological experiments such as sensing. It has been shown that electrodes modified with graphene or graphene-composite can be directly used as

transducers for electrochemical sensing.^[153] Different approaches have been explored for the fabrication of novel biosensors relying on graphene or graphene composites as sensing elements,^[154, 155, 156, 157] yet there is still room for further improvements. In particular, non-covalent functionalization of graphene with ordered 2D arrays of bioactive entities can boost the performance of biosensors and, more generally, be of interest for bio-related applications.

4. Molecule-assisted ultrasound-induced liquid-phase exfoliation

The in-depth understanding over the effect of forces existing between molecules and graphene when they are brought together from the structural and functional point of view is key in order to unravel and control the interactions that can compete to the π - π stacking holding together graphene layers in graphite. In this regard, following the discussion in the Section 2, one of the most effective methods to reduce the strength of the van der Waals interactions between graphene sheets is the liquid immersion, followed by ultrasound-induced liquid-phase exfoliation. As a result, increasing research efforts are being devoted to the production of graphene *via* LPE, and in particular *via* UILPE, with a close look on improving the material's physico-chemical properties. Remarkably, because of its versatility UILPE can be applied to different 2D layered systems,^[59, 60, 158, 159] such as transition metal dichalcogenides (TMDs) exhibiting different composition, e.g. MoS₂, WS₂, NbSe₂, TaS₂, as well as black phosphorus^[160] and graphene-like (hexagonal) structures like *h*-BN,^[161] thereby enabling the tuning of various physico-chemical properties of these materials.

Solvents with surface tension (γ) \sim 40 mJ m⁻²,^[63] are reported to be ideal for dispersing graphene and graphitic flakes, since they minimize the interfacial tension between the graphene and the solvent. Therefore the solvents of choice are very few and include N-Methyl-2-pyrrolidone (NMP; γ - 40 mJ m⁻²), N,N-Dimethylformamide (DMF; γ - 37.1 mJ m⁻²), *ortho*-dichlorobenzene (*o*-DCB; γ - 37 mJ m⁻²),^[63] see Figure 6. Unfortunately, the use of these solvents has some drawbacks that cannot be neglected, e.g. NMP and *o*-DCB can cause

irritation of the eyes and respiratory tract. Furthermore NMP and DMF are toxic for multiple organs.^[162, 163] Because of these reasons, the search of alternative solvents for graphene exfoliation has attracted considerable attention in the past few years.

In 2009 Bourlinos and co-workers^[164] tested the efficiency of a peculiar class of fluorinated solvents. In particular, perfluorinated analogous of hydrocarbon solvents, i.e. benzene, toluene, nitrobenzene, and pyridine, have been employed. The performance of each solvent was reported as follows: octafluorotoluene ~ pentafluoropyridine < hexafluorobenzene < penta fluorobenzonitrile (see Figure 6). The mechanism of stabilization most likely involves charge transfer through π - π stacking between electron-rich graphene sheets and electron-deficient aromatic molecules; the performance of the solvents directly depends on the chemical nature of the solvent molecules, i.e. the strength of electron-withdrawing fluorine atoms. Moreover, depending on the solvent, the concentrations of the graphene dispersions, mostly composed of a few-layered graphene (FLG), ranged between 0.05 and 0.10 mg mL⁻¹. Adamson and co-workers have investigated the use of hexafluorobenzene as UILPE media in 2012,^[165] and they showed that by mixing it with benzene at 1:1 ratio, graphene dispersions characterized by extremely high concentrations (50 mg mL⁻¹) could be obtained.

Recently, Sun^[166] and co-workers have demonstrated that graphene can be successfully dispersed in amine-based solvents, namely 3,3'-iminobis(*N,N*-dimethylpropylamine) (DMPA), *N*-[3-(dimethylamino)propyl]methacrylamide (DMAPMA), 2-(*tert*-butylamino)ethyl methacrylate (BAEMA) and 2-(dimethylamino)ethyl methacrylate (MAEMA), see Figure 6. Molecular dynamics (MD) simulation justified the existence of strong solvent-graphene interactions resulting in small free energy costs by dispersion. Albeit the concentration of graphene dispersions was reported being as high as 15 mg mL⁻¹ (estimated *via* analysis of absorption coefficient), no information on the sheet(s) thickness was given.

Among numerous solvents successfully employed for dispersing graphene, ionic liquids (ILs), molten salts comprising organic and inorganic ions with melting temperatures below 100°C, are gathering substantial attention in the field.^[167] In 2003, Aida and co-workers observed that imidazolium-based ILs could be used for untangling carbon nanotubes (CNTs).^[168] It was concluded that this process relies on overcoming the π - π interactions between CNTs by the use of positive charge of imidazolium ring. Few years later, Han and co-workers reported the use of IL 1-butyl-3-methylimidazolium hexafluorophosphate ([BMIM][PF₆]; see Figure 7) as a solvent to disperse and chemically modify graphene with a polymerized IL.^[169] Noteworthy, the latter example deals with the use of ILs as a media for chemical modification of graphene. Dispersions of unoxidized and unmodified graphene sheets *via* IL-assisted UILPE have been obtained for the first time in 2010 by Wang and co-workers.^[170] In their process, natural graphite flakes were dispersed in 1-butyl-3-methylimidazolium bis(trifluoromethanesulfonyl)amide [BMIM][Tf₂N] (Figure 7), and subjected to tip sonication. X-ray photoelectron spectroscopy (XPS) studies showed the graphene dispersion was stabilized by strong non-covalent interactions of the ILs with the graphene sheets. Following this approach, Mariani and co-workers exfoliated graphene exploiting 1-hexyl-3-methylimidazolium hexafluorophosphate [HMIM][PF₆] (Figure 7) as an IL.^[171] In 2014, Quitevis and co-workers investigated the use of various ILs as a liquid media in UILPE.^[172] Among the four different ILs, the use of 1,3-Bis(phenylmethyl)imidazolium bis(trifluoromethanesulfonyl)amide [(BnzM)₂IM][Tf₂N] (Figure 7) and its asymmetric analogue, 1-phenylmethyl-3-methylimidazolium bis(trifluoromethanesulfonyl)amide [(BnzM)MIM][Tf₂N] resulted in graphene concentration estimated as 5.8 and ~ 0.1 mg mL⁻¹, respectively.

It is important to note that benchmarking values of graphene concentration is one of the biggest matters in the field. The concentration of graphene as well as the lateral flake size differs significantly from one article to another. This can be justified by the fact that different

experimental conditions, such as initial graphite concentration, solvent volume, sonication power and temperature employed by various groups, are (with a few exceptions) commonly omitted or not discussed. Therefore, it is extremely important to define a reproducible protocol relying on the best experimental conditions for the UILPE and in LPE in general, as well as the use of defined standards for describing the graphene dispersions. In particular, the yield of UILPE can be determined as the ratio between the mass of graphene flakes suspended in the liquid and mass of the starting material (Y_w [%]),^[32] or as Y_s [%], i.e. the ratio between the single- and multi-layer flakes in the dispersion. Furthermore, the ratio between the weight of SLG and the total weight multi-layer flakes gives the information about Y_{ws} [%], i.e. the yield by SLG weight. While Y_w can give only qualitative information, Y_s and Y_{ws} are more informative and describe the quality of the dispersions.

In order to fully illustrate the performance of UILPE process and characterize the graphene dispersions, both quantitative and qualitative description have to be presented. The number of graphene layers (N) can be quantified using High Resolution - Transmission Electron Microscopy (HR-TEM)^[32, 63] and Raman spectroscopy.^[69, 70] Together with the information coming from electron diffraction patterns, in HR-TEM the number of layers can be directly counted by analyzing the folded sheet edges.^[173] The N can be also estimated by exploiting AFM imaging. However, it is important to note that SLG height *via* AFM depends on the substrate and on the environmental conditions, especially the relative humidity. Because of different hydrophilic nature of various substrates the thickness of SLG can vary. In particular, on mica SLG thickness amounts to ~ 0.4 nm,^[174] while on SiO₂ SLG appear to have a height of ~ 1 nm,^[43] which is typically ascribed to the water layer being trapped between SLG and SiO₂. Raman spectroscopy makes it possible to identify structural damages, electronic perturbations, as well as non-covalent functionalization and chemical modifications (possibly) taking place during the LPE, processing or deposition of graphene on various substrates.^[175, 176] The analysis of Raman spectra can also provide information on the number

and position of broken-conjugation areas in graphene, known as graphene atomic- or point-defects, which can affect the electronic properties of graphene. Over the past years, there has been a major effort towards the understanding of Raman spectroscopy of graphene, powered by new results on doping,^[177, 178, 179, 180, 181, 182] edge defects,^[183, 184, 185, 186, 187] electrical mobility^[188, 189] and oxidation.^[190]

The use of properly selected organic molecules can enhance the exfoliation of bulk graphite into graphene, in particular when the molecules have a high energy of adsorption on the basal plane of graphene. It is worth noting that these molecules do not act as graphene dispersants or graphene exfoliators, i.e. they do not trigger the exfoliation of the flakes, as commonly misinterpreted in various articles. These molecules mainly act as graphene dispersion-stabilizing agents (DSAs) *via* non-covalent functionalization of graphene, i.e. through the physisorption of their hydrophobic moieties on the graphene surface during the exfoliation of graphite in liquid media. Therefore, DSAs prevent re-aggregation of the exfoliated sheets.

4.1. Aqueous dispersions

Water, the "natural" solvent, has $\gamma \sim 72 \text{ mJ m}^{-2}$,^[191] which is too high ($\sim 30 \text{ mJ m}^{-2}$ higher than NMP) for dispersing graphene and graphite.^[192] Moreover, due to the hydrophobic nature of graphene sheets they tend to re-aggregate in aqueous dispersions. Nevertheless, the use of water as a liquid medium in UILPE of graphite opens perspectives to green chemistry and to the development of graphene-based biocompatible materials.^[193, 194] Remarkably, the low performance of water in UILPE can be overcome by using DSAs molecules to help the exfoliated graphene sheets to remain dispersed and prevent their aggregation.^[195, 196, 197, 198, 199, 200, 201, 202, 203]

4.1.1. Polycyclic aromatic hydrocarbons

Among DSAs, polycyclic aromatic hydrocarbons (PAHs)^[204, 205, 206, 207] substituted with various side groups are the most studied compounds.^[102, 208] Adsorption of PAHs onto the graphene surface occurs *via* π - π interactions between the planar π -conjugated surfaces. In these non-covalent interactions both PAHs and graphene aromatic planar surfaces share the electrons of π -orbitals, ultimately resulting in the reduction of the surface free energy of the dispersion. Hitherto different PAHs have been employed:

Pyrenes:

In the past decade, pyrene derivatives have been successfully used to stabilize CNTs dispersions,^[209] and as in the case of NMP, they have been adopted for UILPE of graphite.^[210, 211, 212, 213, 214, 215, 216, 217, 218] Noteworthy, DSAs suitable for dispersing CNTs with a curved surface may not always be ideal for dispersing graphene with a flat surface. Figure 8 portrays the chemical formulae of different pyrene derivatives used as the DSAs. In particular, in 2010 He and co-workers^[218] dispersed SLG into an aqueous dispersion by exploiting 1,3,6,8-pyrenetetrasulfonic acid tetrasodium salt (Py(SO₃)₄) (see Figure 8) and aminomethylpyrene (PyMeNH₂) as DSAs, and fabricated transparent conductive films. Yet, neither the yield nor the effectiveness of the protocol was discussed, and aggregates likely remained in these dispersions beside the final products. In 2012, a variety of pyrenes were employed by Green and co-workers^[215] to test their performance as DSAs. Among all investigated pyrene derivatives, i.e. Pyrene (Py), 1-Pyrenecarboxylic acid (PyCA), 1-Pyrenebutyric acid (PyBA), 1-Pyrenesulfonic acid hydrate (PySAH), 1-Aminopyrene (PyNH₂), 1-Aminomethyl pyrene (PyMeNH₂), 1-Pyrenebutanol (PyBOH), 1-Pyrenesulfonic acid sodium salt (PySO₃) and 1,3,6,8-Pyrenetetrasulfonic tetra acid tetra sodium salt (Py(SO₃)₄), the PySO₃ was found being the most efficient, yielding graphene dispersion concentration as high as 1 mg mL⁻¹. To quantify the amount of SLG and FLG in the dispersions, the PySO₃-stabilized graphene

samples were characterized by HRTEM, which revealed the presence of 2-4 layers thick sheets, as commonly observed in UILPE samples.

In 2013 Palermo and co-workers^[213] went one step further by investigating the thermodynamics of molecule-assisted UILPE of graphite. In particular, the authors studied the mechanism of physisorption of various pyrenes on graphene surface, and successive UILPE in water. A detailed analysis was performed on pyrenes functionalized with sulfonic groups. In particular, 1-Pyrenesulfonic acid sodium salt (PySO₃), 6,8-Dihydroxy-1,3-pyrenedisulfonic acid disodium salt (Py(OH)₂(SO₃)₂), 8-Hydroxy-1,3,6-pyrenetrisulfonic acid trisodium salt (PyOH(SO₃)₃), and 1,3,6,8-pyrenetetrasulfonic acid tetrasodium salt (Py(SO₃)₄) were tested. Experimental results collaborated with molecular dynamics simulations provided evidence for a correlation between molecule-graphene adsorption energy and the amount of dispersed graphene sheets; for example the potential of mean force (PMF) of the adsorption process within several sampling windows can be seen on Figure 9. Remarkably, the results obtained imply that the performance of pyrene-assisted UILPE is indirectly driven by the molecular dipoles, which are not important *per se*, but since they facilitate the adsorption of pyrenes on graphene sheets, they promote the lateral displacement of the solvent molecules intercalating between the graphene sheets and pyrene cores.

Noteworthy, some other attempts to enhance UILPE of graphite in water by making use of pyrene-graphene π - π interactions have been reported. In 2011, Lee and co-workers^[212] showed that an aromatic amphiphile based on a conformationally flexible aromatic segment including four pyrene units (PyHD), stabilizes graphene dispersions in water with the concentration of 1.5 mg mL⁻¹. In other works Shi,^[219] Müllen,^[202] and Honma^[211] used pyrenebutyrate (PyBA) and/or pyrenesulfonic acid (Py-SAH) to stabilize graphene in water for use in electrochemical, solar cell, and composite applications. The examples above demonstrate that the use of Py molecules enables a rational modification of both the electronic structure and the conductivity of graphene sheets as well as its performance in Li-ion batteries.

Naphthalenes:

Recently, Liu and co-workers^[220] designed a naphthalene diimide (NDI) with ionic groups attached to the NDI unit through flexible alkyl spacers (NDICA in Figure 8) and successfully used it as DSAs. They showed that NDICA exhibit an excellent capability to exfoliate graphite and disperse graphene in an aqueous solution, as revealed by the ability to produce few-layered graphene with concentration as high as 5 mg mL⁻¹ after centrifuging at 1000 rpm or 1.2 mg mL⁻¹ after centrifuging at 5000 rpm. The superior performance of the surfactants is attributed to their chemical structures, which enable strong π - π interactions between NDICA and graphene and electrostatic (ionic) interactions between COO⁻ groups of NDICA and water molecules.

Perylenes:

Several perylene-based DSAs have been used to promote the exfoliation of graphite in aqueous solutions, including sophisticated perylene diimide (PDI)-based bolaamphiphiles^[200, 221] (PDIBBA; Figure 8) and PDI-sulfonic acid (PDI(SO₃)₂).^[202] An effective and efficient method for the preparation of graphene by UILPE in aqueous dispersions, was demonstrated by Stupp, Stoddart and co-workers,^[222] by using N,N'-dimethyl-2,9-diazaperopyrenium dichloride (PDAP; see Figure 8) molecules to stabilize dispersed graphene sheets in water *via* electrostatic repulsion between the positively charged PDAPs physisorbed on graphene flakes.

Aqueous dispersions stabilized by other PAHs:

Because of the good improvement of the UILPE in presence of small polycyclic aromatic hydrocarbons such as pyrenes, NDIs and PDIs acting as DSAs, other PAHs are also expected to be suitable to stabilize graphene produced by the means of UILPE. Not surprisingly, it has been recently demonstrated that both coronene^[201] and anthracene,^[199]

could also be used as DSAs. In particular, Lee and co-workers showed that the exfoliation of graphite can be also attained by non-covalent functionalization using 9-anthracene carboxylic acid (ACA), yielding in FLG dispersions.^[199] Remarkably, ACA-graphene based composite possesses notable electronic properties, i.e. it exhibits high specific capacitance value of 148 F g⁻¹, as demonstrated by fabricating ACA-graphene based ultracapacitor.

4.1.2. Polymers as DSAs

Over the past years, it has been proven that graphene can be dispersed in water by using a wide range of polymers acting as DSAs, ^[14, 195, 197, 198, 215, 216, 217, 223, 224, 225, 226, 227, 228, 229, 230, 231, 232] such as cellulose acetate (CA),^[233] ethyl cellulose (EC),^[229] polyvinylpyrrolidone (PVP),^[224] lignin,^[230] gum arabic (GA),^[225, 226] gelatin derived from animal skin and bones,^[227] and even more complex systems such as bovine serum albumin (BSA),^[223] hyaluronan (PyHA)^[216] and DNA^[198] functionalized with pyrene head-groups.

While majority of DSAs used in UILPE of graphite feature a ionic nature, in their pioneering work Guardia and co-workers,^[228] investigated a variety of nonionic DSAs, and compared them with their ionic analogues. It was concluded that the non-ionic DSAs significantly outperform their ionic counterparts. The best result, being a graphene dispersion of ~1 mg mL⁻¹, was achieved by using the triblock copolymer Pluronic[®] P-123 (see Figure 6). AFM analysis revealed that graphene sheets obtained with P-123 had lateral sizes in the range of hundreds of nanometers, and almost all the sheets were thinner than 5 layers thick (ca. 15% SLG), in accordance with other investigations of DSAs-assisted UILPE.

More recently, Farris and co-workers performed UILPE of graphite in water with the assistance of three polysaccharides, namely nonionic pullulan, cationic chitosan, and anionic alginate.^[232] The effects of polymer type, initial concentration of graphite, and ultrasonication time on the graphene concentration and quality were compared. Upon ultrasonication treatment for 30 min it was possible to produce graphene dispersions with concentrations

reaching 2.3 mg mL^{-1} in pullulan-stabilized dispersions and 5.5 mg mL^{-1} in the case of chitosan. The obtained graphene sheets were characterized as low-defect SLG, and FLG (<5). The findings arising from these studies suggest that pullulan and chitosan are outperforming alginate as DSAs, due to the different surface free energy and thermodynamic affinity.

The use of polymers as DSAs in the UILPE process is unquestionably more beneficial than the use of organic molecules in terms concentration of the obtained graphene dispersion. However, because of the strong polymer/graphene interactions the majority of graphene produced by exploiting this approach cannot be separated from the polymer/graphene composites. Nevertheless, high fraction of polymer can be removed following the approach proposed by Bourlinos and co-workers,^[224] which relies on the use of graphene “bad solvents”. Towards this end, the authors showed that majority of PVP can be removed from the graphene/PVP composite by washing it with ethanol/chloroform mixture followed by centrifugation, yielding in water suspendable PVP-coated graphene sheets.

Interestingly, in some cases the removal of the polymeric DSAs is not required, and in fact their presence can have some advantages. In this framework, Yoon and co-workers have shown that graphene dispersions can be stabilized by four different polymers based on either poly(vinyl alcohol) (PVA) or dextran functionalized with conjugated moieties, such as phenyl or pyrene (see PyDT and PyPVA in Figure 10).^[217] The ability of these polymers to stabilize graphene dispersions was systematically investigated. Moreover, graphene hydrogels and aerogels were prepared from the aqueous dispersion of the graphene/polymer. The cross-linking of the dispersed polymers in the solution yielded hydrogels with embedded graphene flakes inside the polymeric networks, and the subsequent freeze-drying of the hydrogel resulted in an aerogel. Figure 11a shows that the graphene/polymer gel can recover its original shape after a compression of more than 50% in height. Furthermore, a gel electrolyte was demonstrated as a second model application of the graphene/polymer composite (Figure 11b). Compared with a control experiment on a PVA gel electrolyte ($84.2 \pm 5.2 \text{ F g}^{-1}$), the use of

graphene/polymer gel electrolyte ($107.5 \pm 3.1 \text{ F g}^{-1}$) led to higher specific capacitances and long-term cycling stability, a result that was assigned to the fact that graphene embedded into the gel enhances the ionic conductivity of the gel.^[234] These results clearly support the variety of possible applications for graphene/DSAs composites.

4.1.3. Other DSAs

Despite the few examples discussed above, residuals of the PAHs and polymeric DSAs can drastically affect the electrical performance of graphene-based devices. Therefore, the search of inexpensive DSAs that have high stabilization efficiency yet which can be easily removed with minimal environmental impact has attracted a notable attention,^[196, 235, 236, 237, 238, 239, 240, 241, 242, 243, 244] as it holds potential for facilitating the industrialization and application of graphene produced in aqueous dispersions.

Various examples of small DSAs have been reported (see Figure 12), and include urea (U),^[240] sodium salt of flavin mononucleotide (FMNS),^[235] 1H,1H,11H-icosofluor-1-decanol polyglycidyl ether (FAPGE),^[242] amphiphilic compound consisting of alternating phenylene and thienylene subunits (PTPTP),^[241] and (1,3,5-tris[(1E)-2'-(4'-benzoic acid)vinyl]benzene) (Ramizol®).^[244] Recently, Palermo and co-workers^[243] described the UILPE, processing and inclusion in polymer composites of FLG by using indanthrone blue sulphonic acid sodium salt (IBS), a very common industrial dye, and showed that IBS can be used to stabilize FLG dispersions in water. To demonstrate that their method is suitable for applications in composites, graphene/IBS hybrids were processed into PVA, enhancing its electrical conductivity by several orders of magnitude.

In 2014 Chen and co-workers described the UILPE of graphite in water into SLG and FLG exploiting pyridine (P) as DSA.^[237] Conductivity of graphene films prepared by filtration of dispersions was reported being as high as 5100 S cm^{-1} . Moreover, the performance of exfoliated graphene was tested as hole transport layer (HTL) and compared with N,N-

di(naphthalene-1-yl)-N,N-diphenylbenzidine (NPB; commercial HTL; see Figure 13a) in organic light-emitting diode (OLED). As depicted in Figure 13b, unusual negative differential resistance (NDR) occurred in both devices. In Figure 13c the efficiency of luminance in the graphene-based LED device was found to be roughly twice higher than that in the NPB-based one.

The same group has also reported on another DSA, namely imidazole,^[236] which interacts with the exfoliated graphene sheets significantly improving the concentration of graphene dispersion (1 mg mL⁻¹) in water. Graphene film prepared from the exfoliated material exhibited an electrical conductivity of 131.7 S cm⁻¹. Furthermore, an all-solid-state supercapacitor with a new design fabricated using the exfoliated graphene sheets delivered an ultrahigh area capacitance (~72 mF/cm²).

Recently, Francis and co-workers demonstrated fine patterning of graphene by screen printing using a silicon stencil and a high conductivity ink based on graphene dispersions prepared by ethyl cellulose (EC) assisted UILPE in ethanol.^[245] The screen-printed graphene patterns (Figure 14a) on polyimide films exhibited high electrical conductivity of 1.86×10^4 S m⁻¹ and remarkable mechanical flexibility, suitable for electronic applications. With the high-quality and flexible graphene patterns as source and drain electrodes, all-printed electrolyte-gated transistors on flexible substrates displayed desirable transfer and output characteristics, as well as durable operation over many bending cycles (Figure 14e).

Regardless of the exfoliation yields and the stability of graphene aqueous dispersions, the use of water as an exfoliation media is not recommended for the exploitation of graphene in electronic devices such as field-effect transistors (FETs). In particular, the presence of water remaining at the interface with the dielectric substrate can enhance charge-trapping phenomena.^[246] Therefore, the use of DSAs-assisted UILPE in organic solvents has to be explored.

4.2. Graphene dispersions in organic solvents

Despite the increasing interest in the field, the knowledge gathered about the DSA-assisted UILPE of graphite in organic solvents is still relatively poor.^[229, 233, 247, 248, 249, 250, 251, 252, 253] The first reported example dealing with this approach involves the use of 1,2-distearoyl-sn-glycero-3-phosphoethanolamine-N-[methoxy(polyethyleneglycol)-5000] (DSPE-mPEG; Figure 15) molecules in a combination with TBA-inserted oleum-intercalated graphite.^[250] Such a mixture was sonicated in DMF to give homogeneous graphene dispersion, which was further deposited on various transparent substrates, including glass and quartz, by exploiting Langmuir-Blodgett (LB). The one-, two- and three-layer LB films on quartz afforded sheet resistances of 150, 20 and 8 k Ω and transparencies of 93, 88 and 83%, respectively.

Porphyrins are known to interact with various carbon-based materials, such as graphite, CNTs and fullerenes through π - π stacking that takes place between porphyrinic electron-abundant aromatic cores and conjugated surfaces.^[254, 255, 256, 257] Therefore, similar interactions are expected to take place between porphyrins and graphene.^[258, 259] To explore this idea, Jung and co-workers dispersed graphene in the presence of 5,10,15,20-tetraphenyl-(4,11-acetyltioundecyl-oxyphenyl)-21H,23H-porphin (TATPP; Figure 15) in NMP containing organic ammonium ions. It was found that the TATPP-assisted UILPE of graphite could be employed to produce high quality SLG sheets.

Successful UILPE of graphite can be also attained in ethanol by exploiting quinquethiophene-terminated PEG (5TN-PEG) as a DSA. Highly graphene films exhibiting interesting opto-electronic properties were fabricated from the graphene dispersions by vacuum filtration. After washing the surfactant with THF followed by chemical treatment with HNO₃ and SOCl₂, the graphene films exhibited a remarkable light transmittance of 74% at 550 nm combined with a sheet resistance of 0.3 k Ω sq⁻¹ and $\sigma_{dc}/\sigma_{ac} = 3.65$.

Graphene can be directly exfoliated from graphite using UILPE and CTAB (Figure 15) acting as a DSA, as demonstrated by Valiyaveetil and co-workers.^[252] The sheets could be dispersed in common organic solvents such as DMF. The characterization of the flakes by various techniques such as TEM, AFM and SEM, revealed the successful exfoliation of graphite into graphene flakes having an average thicknesses of ~ 1.2 nm. Field emission measurements showed a turn on voltage of $7.5 \text{ V } \mu\text{m}^{-1}$ and emission current densities of 0.15 mA cm^{-2} .

The use of small organic molecules such as DSAs is expected to promote the UILPE of graphite when the DSA molecules have a strong affinity for graphene, being stronger than that of the solvent/graphene interactions. A good starting point in terms of molecular design relies on the use of alkanes which are known to exhibit a high affinity for the basal plane of graphite/graphene.^[99] In this framework, we have recently demonstrated that arachidic acid (C19CA; Figure 15) and *n*-octylbenzene (NOTB) can be successfully exploited to promote the exfoliation of graphene in NMP.^[247] Notably, the addition of the C19CA and/or NOTB does not affect the quality and structure of obtained graphene, as compared to the use of NMP alone, highlighting the non-invasive nature of the process. Furthermore, the use of alkyl chain based DSAs lead to an increase the percentage of SLG and bilayer graphene flakes. In particular, by using NOTB as DSA the amount of SLG increases by ca. 10 % and graphene concentration increases of 25%, with respect to graphene exfoliated in pure NMP. Conversely, the use of C19CA resulted in a slightly lower increase of percentage of SLG and a 50% increase of the concentration.

We have also shown that the performance of linear alkanes exposing a carboxylic acid head group as DSAs directly depends on the length of the linear alkane chain.^[249] Towards this end, we explored five linear modules, i.e. hexanoic acid (C6CA), lauric acid (C12CA), stearic acid (C18CA), lignoceric acid (C24CA) and melissic acid (C30CA) (Figure 15), whose different adsorption energies on graphene and marked tendency to form tightly packed

self-assembled monolayers on such a surface affected their performances as DSAs. The analysis of the carboxylic acid assisted UILPE revealed that the concentration of graphene dispersions prepared in NMP, *o*-DCB and TCB increases linearly with the length of the aliphatic chain (Figure 16). The observed dependence of the UILPE yield with the length of the aliphatic chain has been interpreted by means of a thermodynamic model of molecular self-assembly on graphene. Our analysis shows that the shorter the aliphatic chain, the larger is the (rotational and translational) entropic cost of forming a 2D structure (Figure 16c). These results suggest that a model based on molecular mechanics for the energetics and a statistical mechanic treatment of entropy, could be used to predict the efficiency of supramolecular building blocks as DSAs and guide the chemical design of the next generation of DSAs. Nevertheless a role of kinetics cannot be fully ruled out.

Besides the above examples on the use of simple DSAs in organic solvents, only a limited number of polymers have been exploited to this end in the past years. In particular, through a modelling study, the group of Coleman have predicted that maximal graphene concentration can be reached when the polymer and solvent have similar Hildebrand solubility parameters as the graphene sheets.^[233] Though effective, graphene concentration in the dispersions obtained therein is however often very low, e.g. 0.141 mg mL⁻¹ in cyclohexanone or 0.02 mg mL⁻¹ in THF. The search for suitable polymers acting as DSAs in conventional low-polarity, low-boiling-point organic solvents is thus important to render highly concentrated graphene dispersions of high quality.

It has been shown recently, that the exfoliated graphene in NMP can be stabilized with an acidic solution of the poly(isoprene-*b*-acrylic acid) (PI-*b*-PAA) or poly[styrene-*b*-(2-vinylpyridine)] (PS-*b*-P2VP) block copolymers^[197] (Figure 10). Unfortunately, the thickness of graphitic flakes amounts to 44 nm and 2.5 nm respectively, implying that the PI-*b*-PAA- and/or PS-*b*-P2VP-assisted UILPE protocol needs to be further optimized.

4.2.1. Bi-component graphene/organic active layers

UILPE graphene in the presence of *ad hoc* molecules can be successfully exploited as a bi-component graphene/organic hybrid active layer for tuning the charge transport in OFETs.^[260, 261] A viable method to address this approach consists in the use of a blend of graphene and an organic/polymeric semiconductor by choosing a liquid media that can act as good solvent for both.

We have recently demonstrated that graphene prepared by UILPE in *o*-DCB can be used in thin-film devices once co-deposited with a polymeric semiconductor in order to boost the ambipolar character of the latter.^[261] In particular, we have shown that the field-effect mobility of holes can be enhanced by 45 folds at the blend ratio 150:1 in weight of poly [*N,N*-9-*bis*(2-octyldodecyl)- naphthalene-1,4,5,8-*bis*(dicarboximide)-2,6-*diyl*]-*alt*-5,5'- (2,2'-bithiophene)], P(NDI2OD-T2), Polyera ActivInk N2200) to graphene, suggesting a favourable pathway for the charge transport. This strategy combining the high performance of a 2D material and the ideal film forming ability of a polymer provides a prospective pathway for the application of graphene in electronics requiring ambipolar devices for complimentary logic circuits.

It is however important to note that blends feature mayor drawbacks such as phase segregation,^[261] graphene random aggregation,^[262] cristallinity loss in the semiconductor matrix^[263] and very poor control over graphene deposition.^[264]

In 2015 we have demonstrated^[265] an alternative strategy to fabricate multifunctional graphene-polymer hybrid thin-film transistors (PG-TFT) whose transport properties are tunable by varying the deposition conditions of graphene dispersions prepared by the means of UILPE of graphite in NMP. It is a multistep procedure characterized by the deposition of a graphene ink on SiO₂ followed by a thermal annealing process in order to fully evaporate the NMP solvent, and the successive deposition of the polymeric semiconductor *via* spin-coating. In particular, we found out that the ionization energy (IE) of graphene films drop-cast on SiO₂

can be finely adjusted prior to polymer deposition *via* thermal annealing in air environment, exhibiting values gradually changing from 4.8 up to 5.7 eV. Such a tunable graphene's IE determines its dramatically different electronic interactions with the semiconducting polymer (*p*- or *n*-type) sitting on its top, leading to devices where the output current of the PG-TFT can be operated from being completely turned off up to modifiable. Moreover, the PG-TFT based on fine energy level engineering, represents a memory device operating without the need of a dielectric layer separating a floating gate from the active channel.

5. Conclusion

In this review article we have shown that the non-covalent functionalization of graphene with ordered supramolecular architectures is a viable approach to decorate surfaces and interfaces with functional molecules and it also opens promising paths to tune the graphene properties. Hitherto, the (supra)molecular approach to graphene is a rather unexplored realm. In order to finely tune the electronic properties of graphene, and especially to modulate its doping, it is crucial to design molecular building blocks that are capable to undergo controlled self-assembly on graphene forming ordered nanopatterns. Depositing simple molecules or layers of self-assembled species, suited for modifying interfacial electronic interactions, on graphene surface cause the interstitial doping by charge transfer processes between supramolecular architectures and graphene, which subsequently results in a modulation of the graphene's work function.

Moreover, when exploited in the liquid phase, this supramolecular approach can be used to harness the performance of ultrasound-induced liquid-phase exfoliation of bulk graphite, a method which is particularly mild, versatile and potentially up-scalable. UILPE in the presence of a given solvent molecule with the aid of an additional molecule acting as an DSA is a path not only to avoid graphene re-aggregation due to van der Waals attraction, but also to increase exfoliation efficiency, thereby compromising the effort made during exfoliation.

Moreover, the presence of the DSAs interacting with the graphene through non-covalent forces can be used to modulate the properties of the graphene by imparting new functions to the 2D material. UILPE approach is extremely interesting from technological point of view as many applications rely on large-scale mass production using low-cost methods such as ink-jet and screen-printing or R2R. UILPE is attractive for the preparation of stable graphene inks that can be processed in thin conductive films and composites. Considerable effort has been made to enhance the degree and the yield of UILPE of graphene. Yet, the yield of SLG sheets is still moderately low and requires long treatment with ultrasound. Additionally, the exfoliated material has quite an amount of graphitic waste, which adds another (purification) step into the UILPE process. In order to leverage the yield and reduce the by-products, various alternative methods are being intensively explored. Amongst the LPE approaches electrochemical exfoliation (ELPE) emerged in the last years as the most promising tactic to disperse graphene in liquid media.^[52] Differently from UILPE, ELPE may cause the edge-oxidation of graphene flakes; however, the level of oxidation is still markedly lower than that of rGO. Moreover, the concentration of dispersion produced by ELPE can be as high as 50 mg mL⁻¹, being two orders of magnitude greater than the average concentration of UILPE dispersions.

Supramolecular approaches to graphene, and supramolecular chemistry itself relies on the use of non-covalent forces to steer the self-assembly of molecular building blocks, with a sub-nanometer precision, to generate materials with well-defined physical and chemical properties. Nevertheless, the labile nature of non-covalent forces defines the stability of the self-assembled structures, which in particular in liquid media is limited, and this thereby jeopardizes the technological exploitation of non-covalently modified graphene. In this regard, covalent attachment of organic molecules onto the basal plane of graphene, and in particular graphene oxide, is being widely investigated, as it appears as relatively more robust than non-covalent functionalization.^[266, 267, 268, 269, 270, 271, 272, 273, 274] Achieving a higher control over the

covalent functionalization of graphene and graphene oxide will be key, as it will allow decorating this wonder 2D material with *ad hoc* functional groups ideally in pre-defined positions to promote inter-sheet interactions *via* non-covalent forces. Design and manipulation of advanced porous 3D graphene-based materials^[275] is another, yet extremely important issue to be considered as the implementation of graphene in 3D well-ordered nanostructures shows a promise in various technologically relevant applications in membranes,^[276, 277] supercapacitors,^[278, 279, 280, 281, 282] fuel cells,^[283, 284] and drug delivery^[285, 286]. To this end, beside the extensive use of π - π interactions, two other non-covalent forces featuring greater geometrical control such as H-bonding and metallo-ligand interactions will be precious tools to improve the structural and functional complexity of graphene based materials. This will allow extending the dimensionality from 2D to 3D to create, even under thermodynamic control, highly ordered composites with tunable porosity for energy applications.

Acknowledgements

We are grateful to Sébastien Haar, Thomas Mosciatti, Mirella El Gemayel, Markus Döbbelin, Jeffrey Mativetsky, Emanuele Orgiu, Emanuele Treossi, Andrea Liscio and Vincenzo Palermo for the joint research activity on graphene chemistry, which was an essential source of inspiration for this review. We acknowledge financial support from the European Commission through the Graphene Flagship (GA-604391), the Agence Nationale de la Recherche through the LabEx project Chemistry of Complex Systems (ANR-10-LABX-0026_CSC) and the International Center for Frontier Research in Chemistry (icFRC).

Received: ((will be filled in by the editorial staff))

Revised: ((will be filled in by the editorial staff))

Published online: ((will be filled in by the editorial staff))

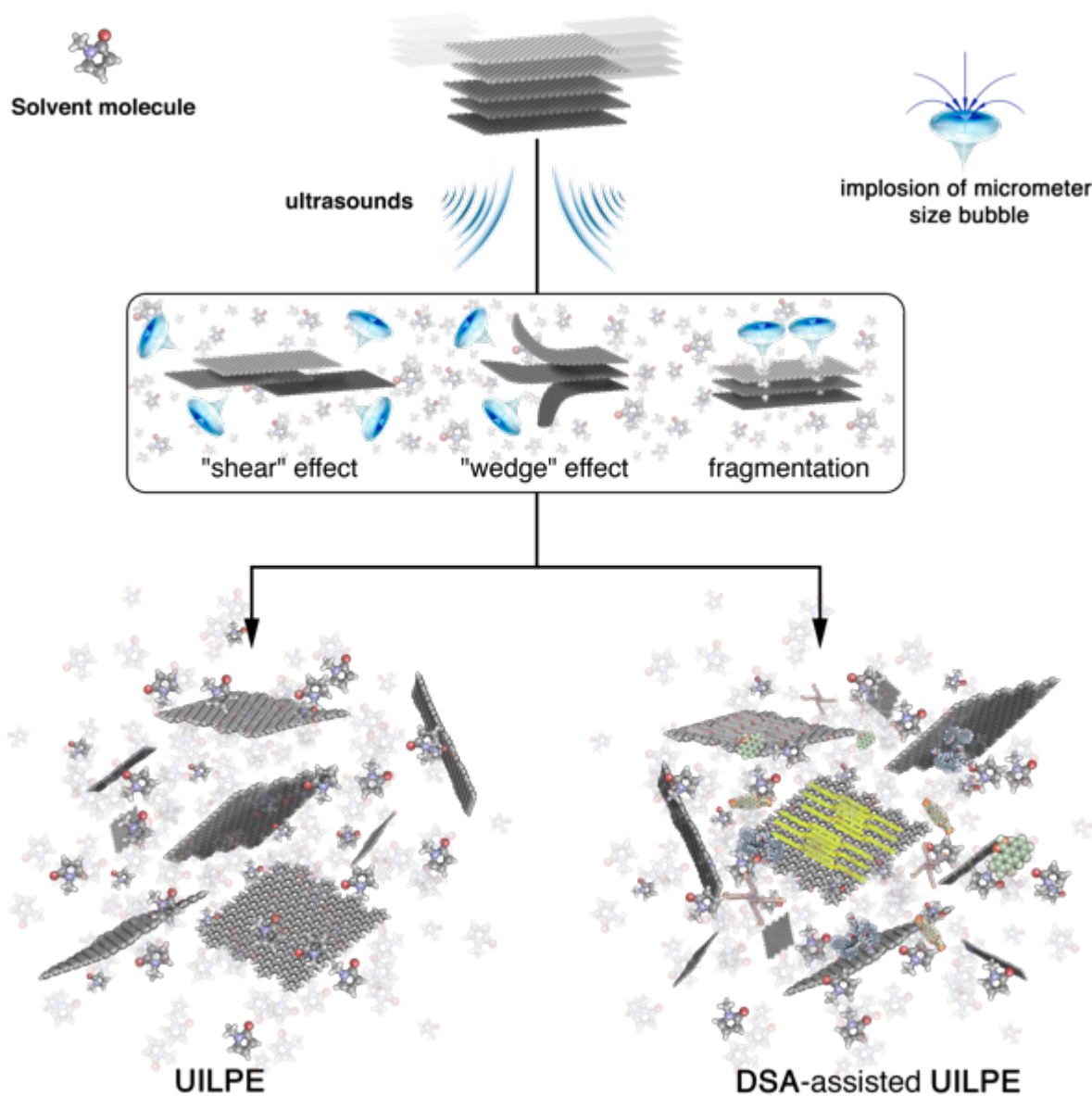


Figure 1. Schematic representation of the ultrasound-induced liquid-phase exfoliation (UILPE) process of graphite in the absence and presence of dispersion stabilizing agents (DSAs).

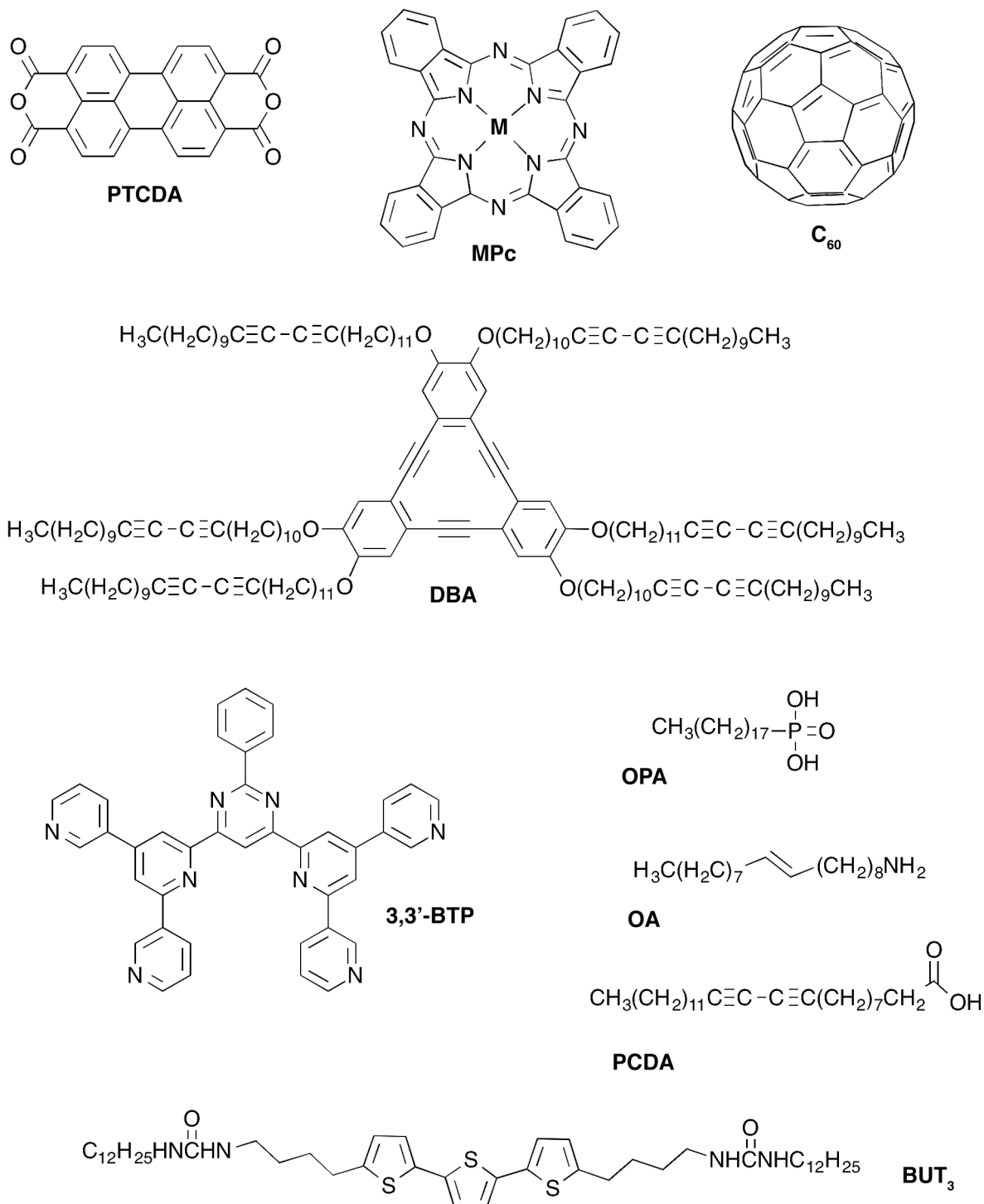


Figure 2. Chemical structure of the molecules used for non-covalent functionalization of graphene, with their acronyms as used in the text.

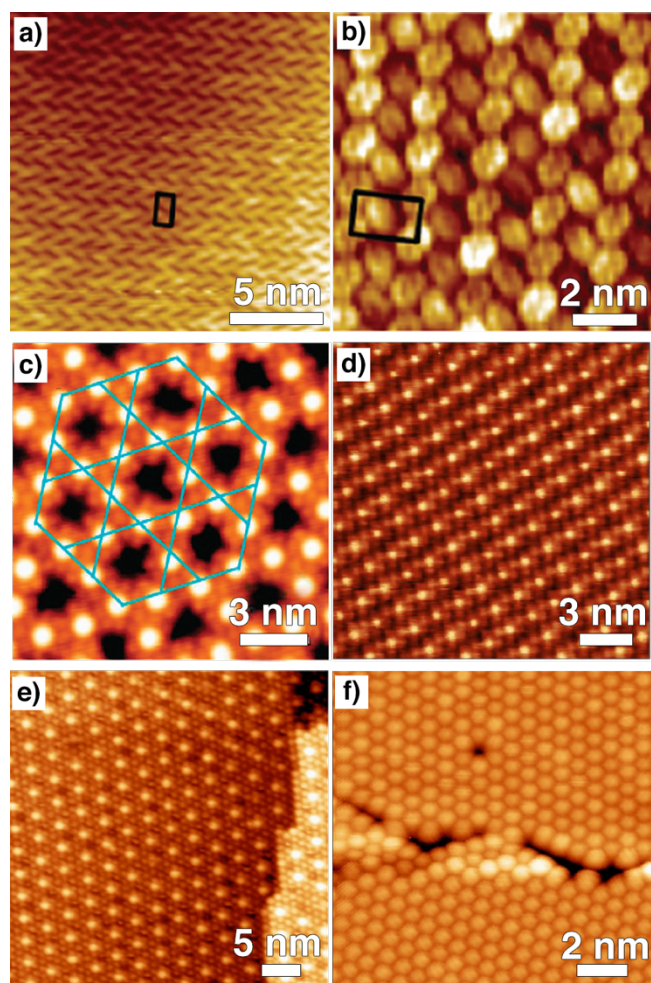


Figure 3. STM images of graphene non-covalently functionalized with PTCDA, Pc and C_{60} molecules. a-b) PTCDA herringbone structure self-assembled on EG/SiC(0001); c) Kagome structure obtained after deposition of FePc on SLG/Ru(0001); d) Square lattice of CoPc self-assembled in MEG/Ir(111); e-f) STM images of C_{60} molecules self-assembled on SLG/Ru(0001) (e) and SLG/SiC (f). Images reproduced from Ref.^[123] (a-b), Ref.^[133] (c), Ref.^[138] (d) and Ref.^[146] (f) with the permission from the American Chemical Society; e) Reproduced from Ref.^[144] with the permission from the American Institute of Physics.

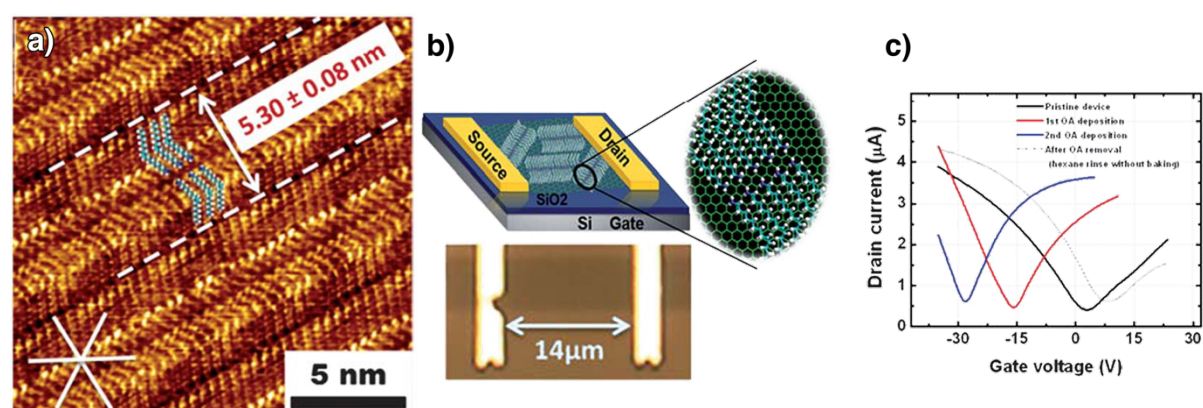


Figure 4. a) STM image of OA molecules self-assembled on HOPG; b) Schematic representation of the G-FET device decorated with self-assembled OA molecules and an optical micrograph of the G-FET; c) I_{ds} - V_g characteristics of a G-FET device before and after several OA treatments and after OA removal taken at a source–drain bias (V_{ds}) of 5 mV under

ambient conditions. Reproduced from Ref.^[150] with the permission from the Royal Society of Chemistry.

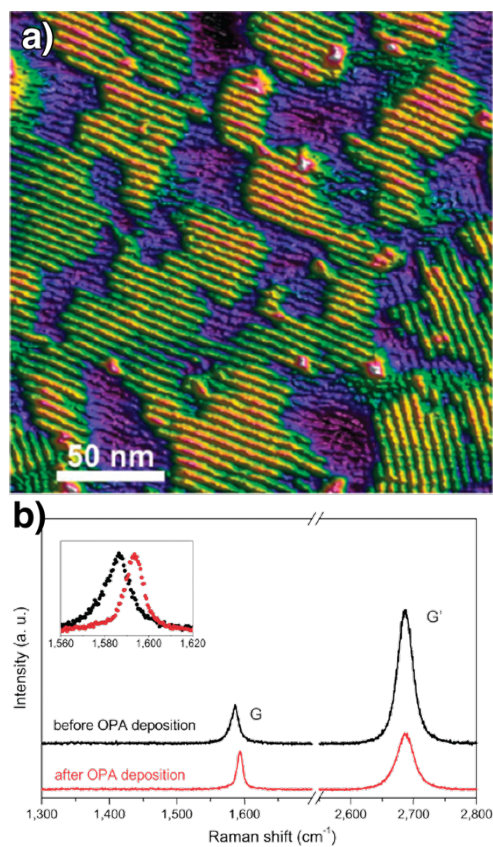


Figure 5. a) AFM topography image of the OPA self-assembled architecture (yellow-green) partially covering graphene surface (blue); b) Raman spectra obtained on graphene and on the OPA-functionalized graphene showing *p*-type doping. Reproduced from Ref.^[151] with the permission from the American Chemical Society.

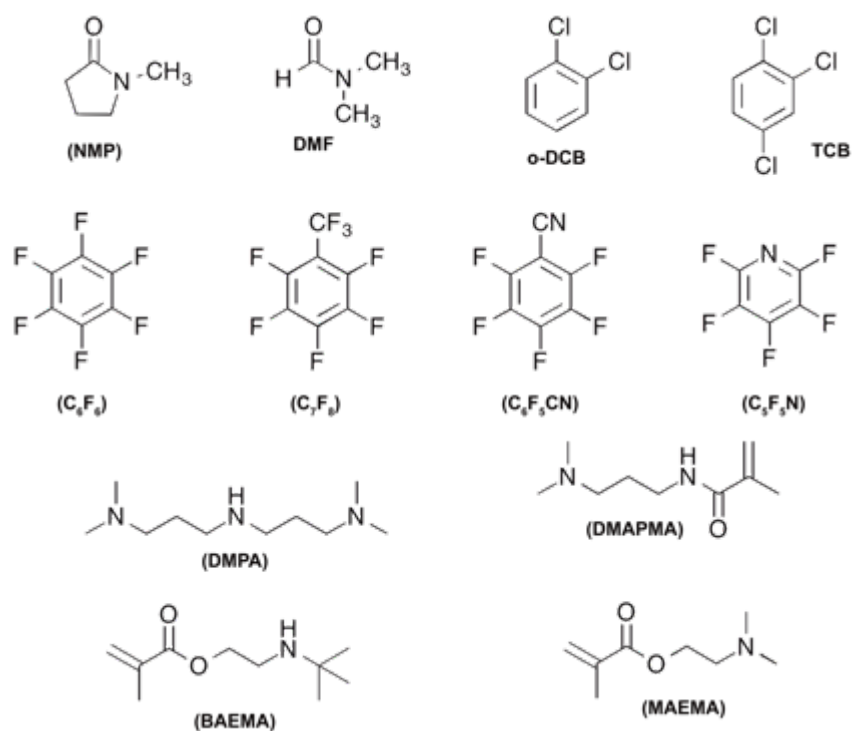


Figure 6. Chemical structure of the solvent molecules used as liquid media in the UILPE process, with their acronyms as used in the text

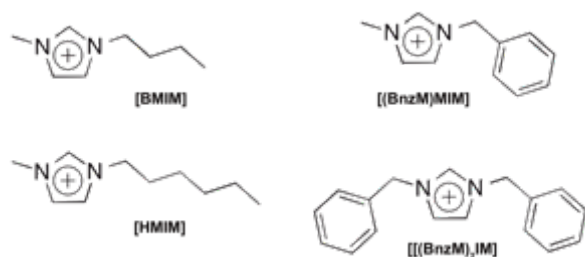


Figure 7. Chemical structure of the ionic liquids (ILs) used as the solvents in the ULPE process, with their acronyms as used in the text.

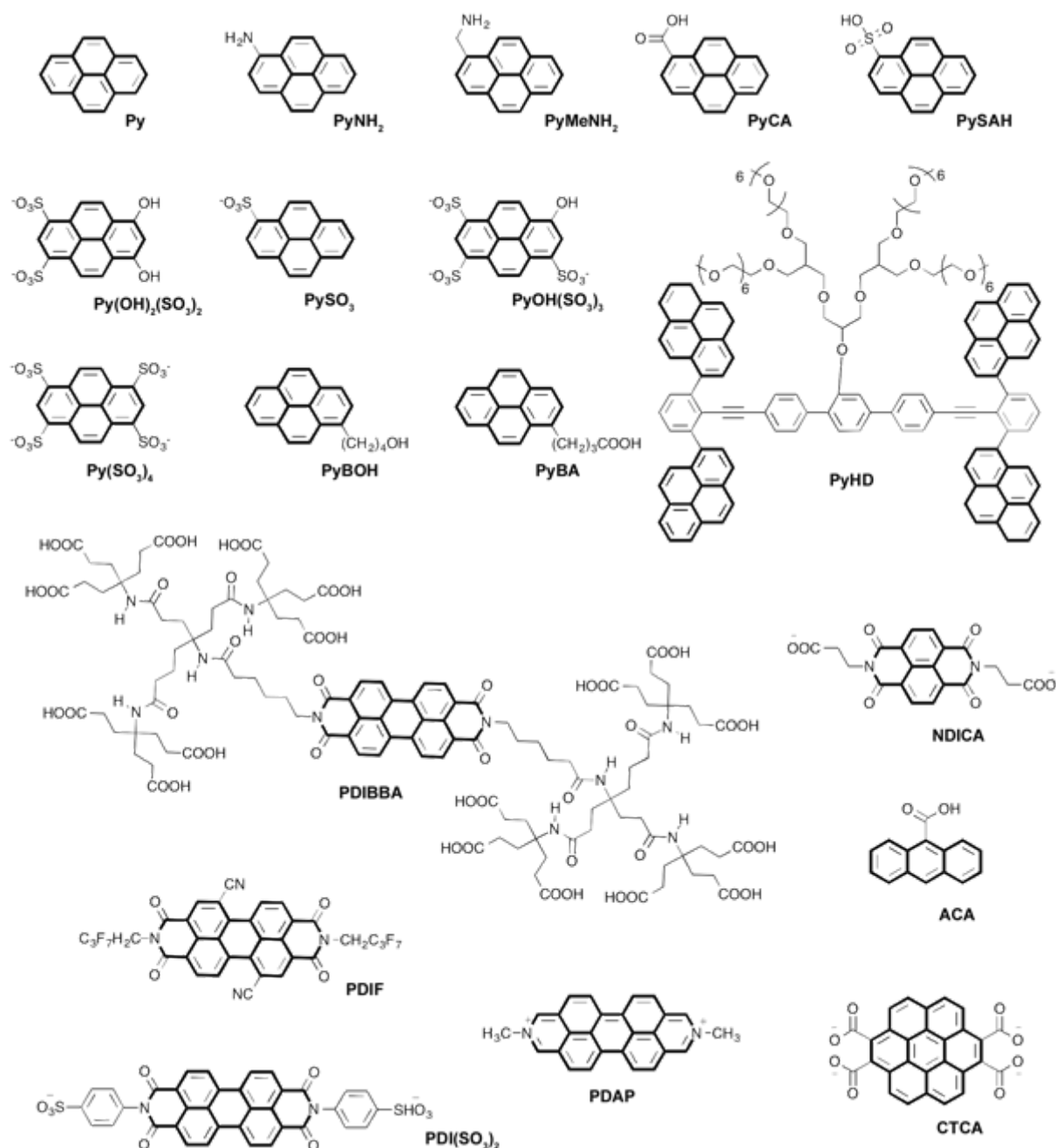


Figure 8. Chemical structure of functionalized polycyclic aromatic hydrocarbons (PAHs) used as DSAs in the UILPE process, with their acronyms as used in the text.

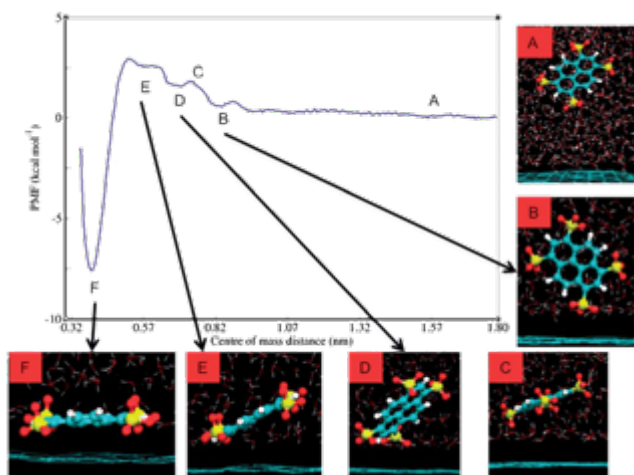


Figure 9. The curve of the potential of mean force (PMF) of $(\text{Py}(\text{SO}_3)_4)$. Snapshots of equilibrium structures at different distances are also shown corresponding to the points on the curve indicated by letters. Reproduced from Ref.^[213] with the permissions from Royal Chemical Society.

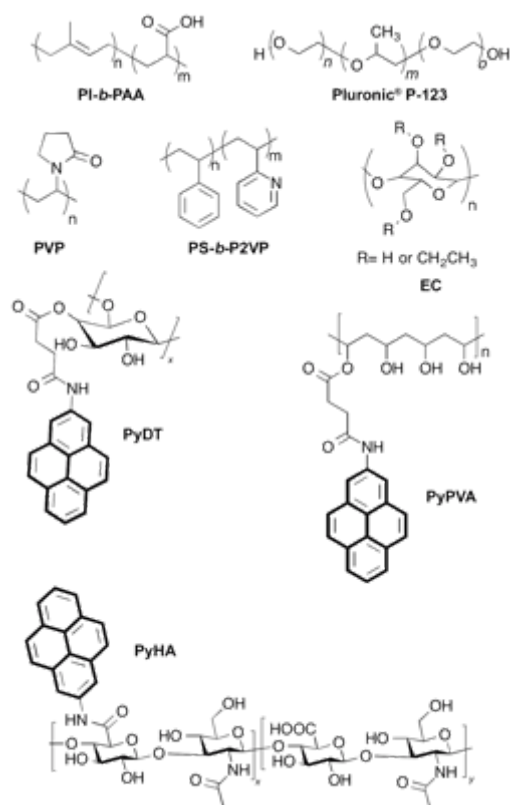


Figure 10. Chemical structure of polymeric DSAs used in the UILPE process, with their acronyms as used in the text.

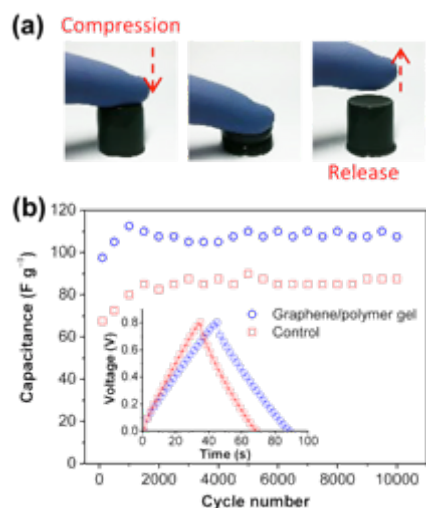


Figure 11. a) Photographs of the compression and release process of aerogels prepared from an aqueous dispersion of graphene/Py-PVA; b) Typical galvanostatic charge/discharge curves (inset) of the solid-state supercapacitor cells recorded at a current density of 0.5 A g^{-1} and their long-term cycling performances. Reproduced from Ref.^[217] with the permissions from the American Chemical Society.

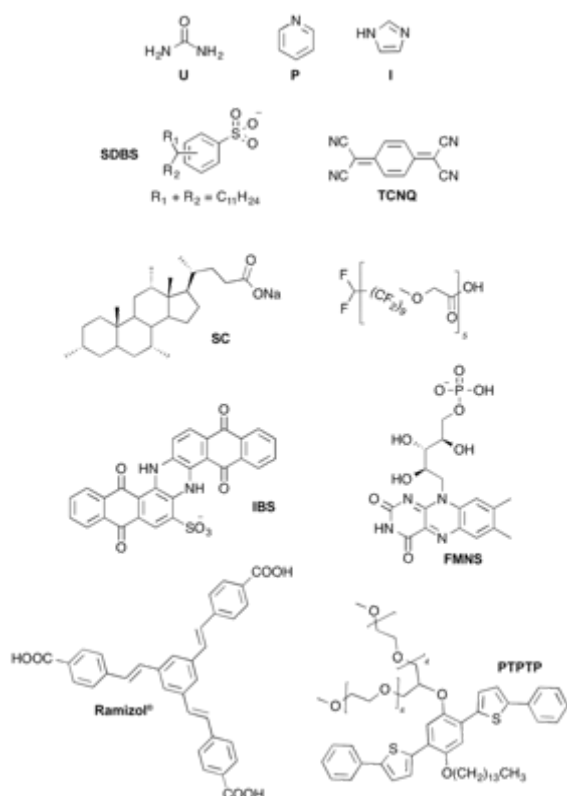


Figure 12. Chemical structure of small organic DSAs used in the UILPE process in water, with their acronyms as used in the text.

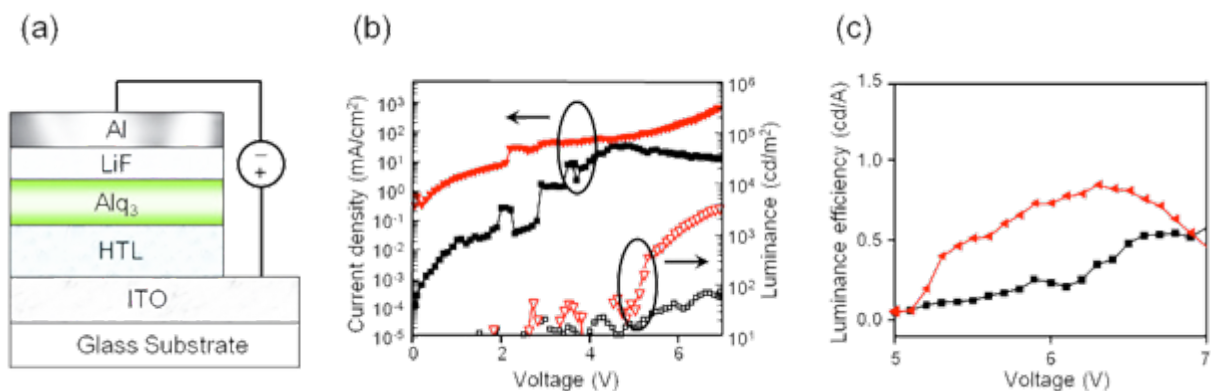


Figure 13. Schematic representation of the hole-transport process in an OLED from a graphene hole transport layer as an alternative to a conventional NPB HTL. (b) Current density-voltage, luminance-voltage, and (c) luminance efficiency-voltage characteristics of an NPB-LED and graphene-LED. (red: graphene-LED; black: NPB-LED). Reproduced from Ref.^[237] with the permission of Nature publishing group.

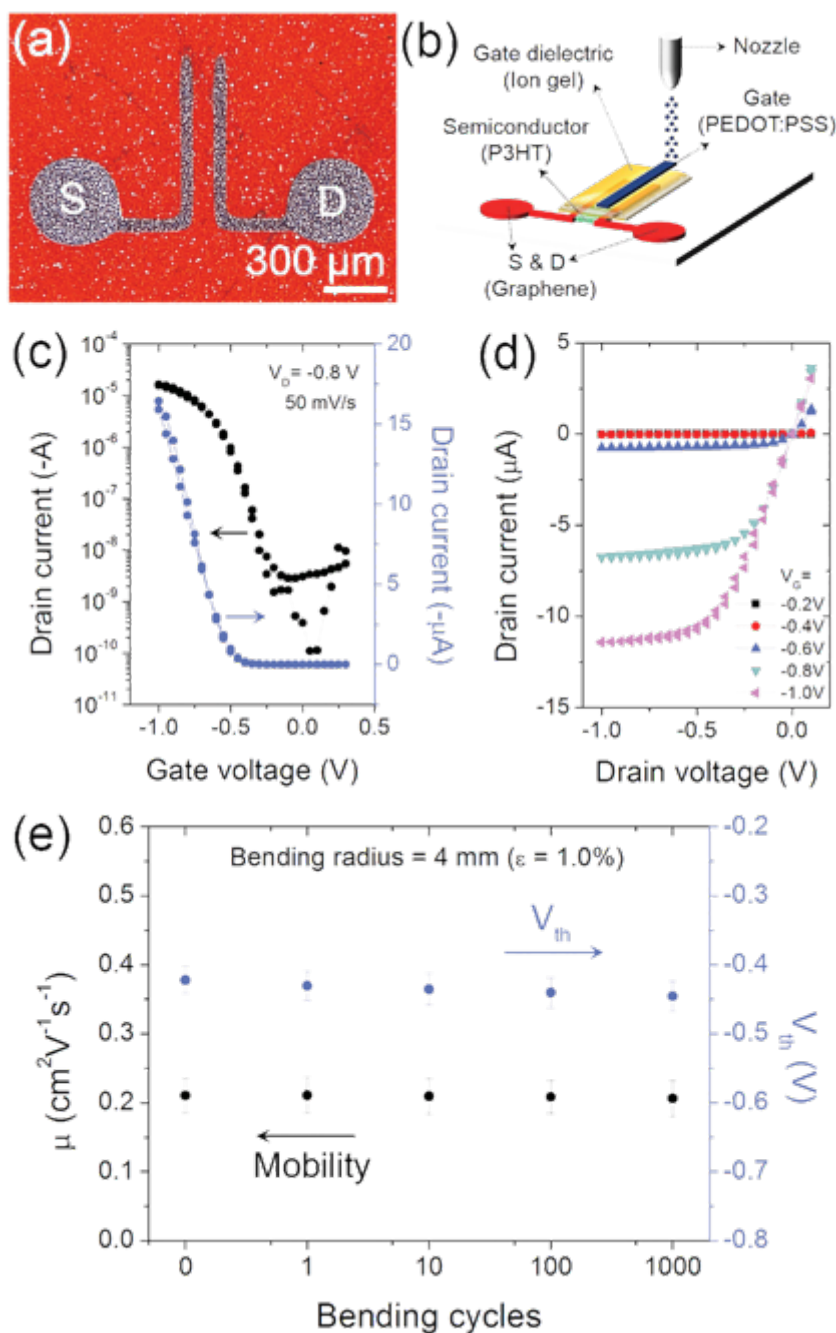


Figure 14. a) Optical microscope image of screen-printed graphene source and drain electrodes on a polyimide substrate for EGTs ($W/L = 900\ \mu\text{m}/90\ \mu\text{m}$). b) Schematic illustration for the EGT architecture fabricated on the graphene electrodes. c) Transfer and d) output characteristics of the printed EGTs. The voltage sweep rate was $50\ \text{mV s}^{-1}$. e) Stability of charge carrier mobility (μ) and threshold voltage (V_{th}) for the EGTs during repeated bending cycles with a bending radius of $4\ \text{mm}$, corresponding to 1.0% strain. Reproduced from Ref.^[245] with the permissions from Wiley-VCH.

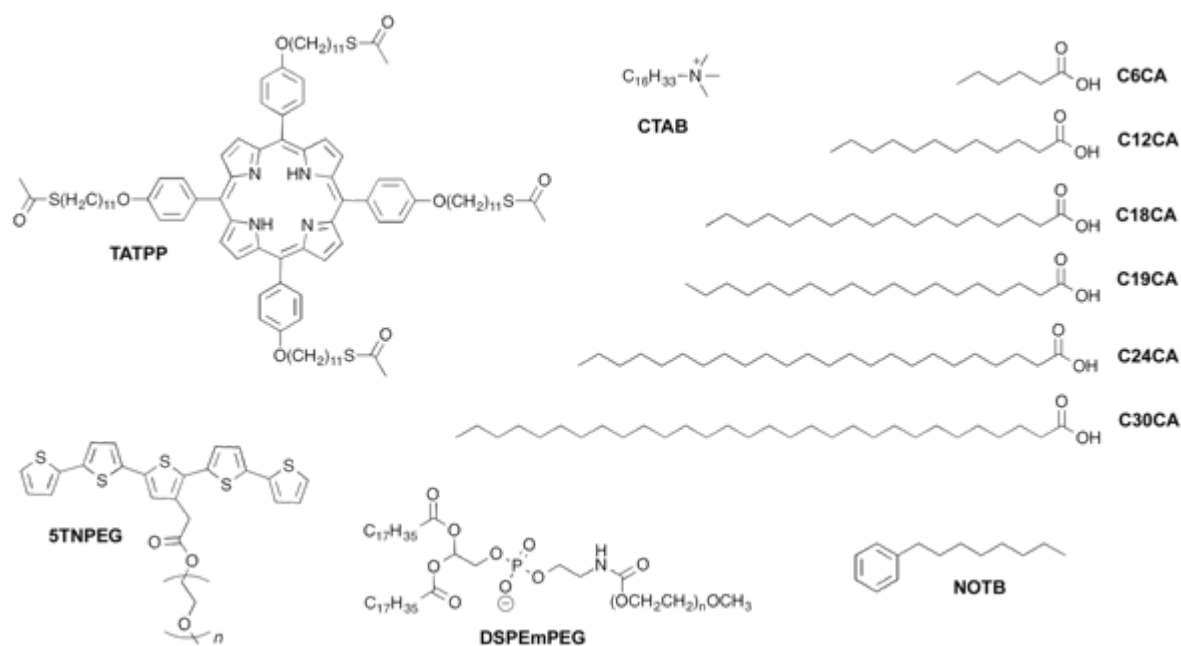


Figure 15. Chemical structures of organic molecules used as DSAs in the process of UILPE of graphite towards graphene in organic solvents, with their acronyms as used in the text.

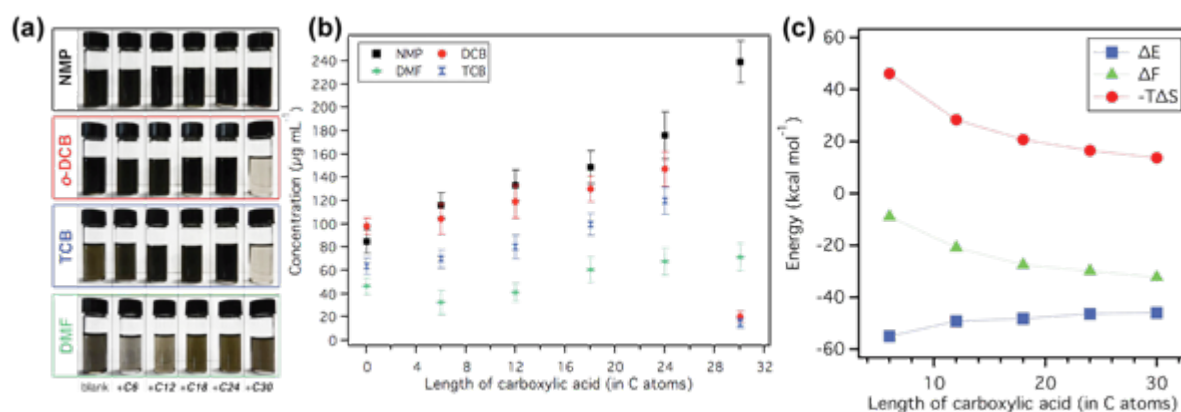


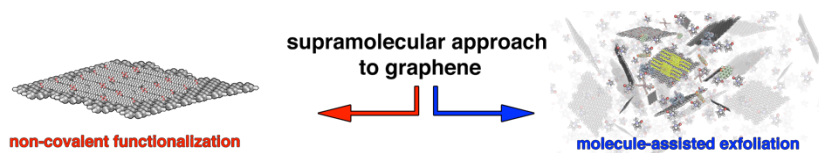
Figure 16. a) Photographs of graphene dispersions prepared by carboxylic acid assisted UILPE of graphite in NMP, *o*-DCB, TCB, and DMF; b) average concentration of graphene dispersions after the filtration process; c) Plot of the internal energy gain (ΔE), entropy cost ($-T\Delta S$), and free energy difference (ΔF) for the five investigated carboxylic acids. Reproduced from Ref.^[249] with the permissions from Wiley-VCH.

Non-covalent functionalization of graphene relies on the use of principles of supramolecular chemistry and can be used to finely tune graphene properties and enhance its production by the means of molecule-assisted liquid-phase exfoliation.

Graphene

A. Ciesielski* and P. Samori*

Supramolecular approaches to graphene: From self-assembly to molecule assisted liquid-phase exfoliation



- [1] A. K. Geim, K. S. Novoselov, *Nat. Mater.* **2007**, *6*, 183.
- [2] A. C. Ferrari, F. Bonaccorso, V. Fal'ko, K. S. Novoselov, S. Roche, P. Boggild, S. Borini, F. H. L. Koppens, V. Palermo, N. Pugno, J. A. Garrido, R. Sordan, A. Bianco, L. Ballerini, M. Prato, E. Lidorikis, J. Kivioja, C. Marinelli, T. Ryhanen, A. Morpurgo, J. N. Coleman, V. Nicolosi, L. Colombo, A. Fert, M. Garcia-Hernandez, A. Bachtold, G. F. Schneider, F. Guinea, C. Dekker, M. Barbone, Z. P. Sun, C. Galiotis, A. N. Grigorenko, G. Konstantatos, A. Kis, M. Katsnelson, L. Vandersypen, A. Loiseau, V. Morandi, D. Neumaier, E. Treossi, V. Pellegrini, M. Polini, A. Tredicucci, G. M. Williams, B. H. Hong, J. H. Ahn, J. M. Kim, H. Zirath, B. J. van Wees, H. van der Zant, L. Occhipinti, A. Di Matteo, I. A. Kinloch, T. Seyller, E. Quesnel, X. L. Feng, K. Teo, N. Rupesinghe, P. Hakonen, S. R. T. Neil, Q. Tannock, T. Lofwanderer, J. Kinaret, *Nanoscale* **2015**, *7*, 4598.
- [3] Z. Li, Z. Liu, H. Y. Sun, C. Gao, *Chem. Rev.* **2015**, *115*, 7046.
- [4] X. Wang, L. J. Zhi, K. Müllen, *Nano Lett.* **2008**, *8*, 323.
- [5] J. D. Roy-Mayhew, I. A. Aksay, *Chem. Rev.* **2014**, *114*, 6323.
- [6] J. B. Wu, M. Agrawal, H. A. Becerril, Z. N. Bao, Z. F. Liu, Y. S. Chen, P. Peumans, *Acs Nano* **2010**, *4*, 43.
- [7] T. Mueller, F. N. A. Xia, P. Avouris, *Nat. Photonics* **2010**, *4*, 297.
- [8] F. N. Xia, T. Mueller, Y. M. Lin, A. Valdes-Garcia, P. Avouris, *Nat. Nanotechnol.* **2009**, *4*, 839.
- [9] T. J. Echtermeyer, L. Britnell, P. K. Jasnós, A. Lombardo, R. V. Gorbachev, A. N. Grigorenko, A. K. Geim, A. C. Ferrari, K. S. Novoselov, *Nat. Commun.* **2011**, *2*, 458.
- [10] G. Konstantatos, M. Badioli, L. Gaudreau, J. Osmond, M. Bernechea, F. P. G. de Arquer, F. Gatti, F. H. L. Koppens, *Nat. Nanotechnol.* **2012**, *7*, 363.
- [11] S. Bae, H. Kim, Y. Lee, X. F. Xu, J. S. Park, Y. Zheng, J. Balakrishnan, T. Lei, H. R. Kim, Y. I. Song, Y. J. Kim, K. S. Kim, B. Ozyilmaz, J. H. Ahn, B. H. Hong, S. Iijima, *Nat. Nanotechnol.* **2010**, *5*, 574.
- [12] E. W. Hill, A. K. Geim, K. Novoselov, F. Schedin, P. Blake, *IEEE Trans. Magn.* **2006**, *42*, 2694.
- [13] N. Tombros, C. Jozsa, M. Popinciuc, H. T. Jonkman, B. J. van Wees, *Nature* **2007**, *448*, 571.
- [14] T. Hasan, F. Torrisi, Z. Sun, D. Popa, V. Nicolosi, G. Privitera, F. Bonaccorso, A. C. Ferrari, *Phys. Status Solidi B* **2010**, *247*, 2953.
- [15] Z. P. Sun, T. Hasan, F. Torrisi, D. Popa, G. Privitera, F. Q. Wang, F. Bonaccorso, D. M. Basko, A. C. Ferrari, *Acs Nano* **2010**, *4*, 803.
- [16] W. R. Yang, K. R. Ratinac, S. P. Ringer, P. Thordarson, J. J. Gooding, F. Braet, *Angew. Chem. Int. Ed.* **2010**, *49*, 2114.
- [17] M. D. Stoller, S. J. Park, Y. W. Zhu, J. H. An, R. S. Ruoff, *Nano Lett.* **2008**, *8*, 3498.
- [18] C. N. R. Rao, A. K. Sood, K. S. Subrahmanyam, A. Govindaraj, *Angew. Chem. Int. Ed.* **2009**, *48*, 7752.
- [19] F. Bonaccorso, L. Colombo, G. H. Yu, M. Stoller, V. Tozzini, A. C. Ferrari, R. S. Ruoff, V. Pellegrini, *Science* **2015**, 347.
- [20] K. F. Chen, S. Y. Song, F. Liu, D. F. Xue, *Chem. Soc. Rev.* **2015**, *44*, 6230.
- [21] W. Luo, Y. Y. Feng, C. Qin, M. Li, S. Li, C. Cao, P. Long, E. Liu, W. Hu, K. Yoshino, W. Feng, *Nanoscale* **2015**, *7*, 16214.
- [22] S. Patchkovskii, J. S. Tse, S. N. Yurchenko, L. Zhechkov, T. Heine, G. Seifert, *Proc. Natl. Acad. Sci. U.S.A.* **2005**, *102*, 10439.
- [23] F. Schedin, A. K. Geim, S. V. Morozov, E. W. Hill, P. Blake, M. I. Katsnelson, K. S. Novoselov, *Nat. Mater.* **2007**, *6*, 652.

- [24] V. Dua, S. P. Surwade, S. Ammu, S. R. Agnihotra, S. Jain, K. E. Roberts, S. Park, R. S. Ruoff, S. K. Manohar, *Angew. Chem. Int. Ed.* **2010**, *49*, 2154.
- [25] G. V. Dubacheva, C. K. Liang, D. M. Bassani, *Coord. Chem. Rev.* **2012**, *256*, 2628.
- [26] P. Avouris, Z. H. Chen, V. Perebeinos, *Nat. Nanotechnol.* **2007**, *2*, 605.
- [27] J. S. Wu, W. Pisula, K. Müllen, *Chem. Rev.* **2007**, *107*, 718.
- [28] K. Müllen, J. P. Rabe, *Acc. Chem. Res.* **2008**, *41*, 511.
- [29] G. Eda, M. Chhowalla, *Nano Lett.* **2009**, *9*, 814.
- [30] G. M. Scheuermann, L. Rumi, P. Steurer, W. Bannwarth, R. Mülhaupt, *J. Am. Chem. Soc.* **2009**, *131*, 8262.
- [31] J. Albero, H. Garcia, in *Advanced Catalytic Materials*, 1 ed. (Eds.: A. Tiwari, S. Titinchi), John Wiley & Sons, New Jersey, and Scrivener Publishing LLC, Salem, Massachusetts, **2015**, pp. 69.
- [32] F. Bonaccorso, A. Lombardo, T. Hasan, Z. P. Sun, L. Colombo, A. C. Ferrari, *Mater. Today* **2012**, *15*, 564.
- [33] D. G. Papageorgiou, I. A. Kinloch, R. J. Young, *Carbon* **2015**, *95*, 460.
- [34] C.-A. Palma, P. Samori, *Nature Chem.* **2011**, *3*, 431.
- [35] L. Chen, Y. Hernandez, X. L. Feng, K. Müllen, *Angew. Chem. Int. Ed.* **2012**, *51*, 7640.
- [36] A. Narita, X. L. Feng, Y. Hernandez, S. A. Jensen, M. Bonn, H. F. Yang, I. A. Verzhbitskiy, C. Casiraghi, M. R. Hansen, A. H. R. Koch, G. Fytas, O. Ivasenko, B. Li, K. S. Mali, T. Balandina, S. Mahesh, S. De Feyter, K. Müllen, *Nature Chem.* **2014**, *6*, 126.
- [37] K. S. Kim, Y. Zhao, H. Jang, S. Y. Lee, J. M. Kim, K. S. Kim, J. H. Ahn, P. Kim, J. Y. Choi, B. H. Hong, *Nature* **2009**, *457*, 706.
- [38] X. S. Li, W. W. Cai, J. H. An, S. Kim, J. Nah, D. X. Yang, R. Piner, A. Velamakanni, I. Jung, E. Tutuc, S. K. Banerjee, L. Colombo, R. S. Ruoff, *Science* **2009**, *324*, 1312.
- [39] C. Berger, Z. M. Song, X. B. Li, X. S. Wu, N. Brown, C. Naud, D. Mayou, T. B. Li, J. Hass, A. N. Marchenkov, E. H. Conrad, P. N. First, W. A. de Heer, *Science* **2006**, *312*, 1191.
- [40] Y. Lee, S. Bae, H. Jang, S. Jang, S. E. Zhu, S. H. Sim, Y. I. Song, B. H. Hong, J. H. Ahn, *Nano Lett.* **2010**, *10*, 490.
- [41] M. Yi, Z. G. Shen, *J. Mat. Chem. A* **2015**, *3*, 11700.
- [42] M. Z. Cai, D. Thorpe, D. H. Adamson, H. C. Schniepp, *J. Mater. Chem.* **2012**, *22*, 24992.
- [43] K. S. Novoselov, D. Jiang, F. Schedin, T. J. Booth, V. V. Khotkevich, S. V. Morozov, A. K. Geim, *Proc. Natl. Acad. Sci. U.S.A.* **2005**, *102*, 10451.
- [44] W. F. Zhao, M. Fang, F. R. Wu, H. Wu, L. W. Wang, G. H. Chen, *J. Mater. Chem.* **2010**, *20*, 5817.
- [45] V. Leon, M. Quintana, M. A. Herrero, J. L. G. Fierro, A. de la Hoz, M. Prato, E. Vazquez, *Chem. Commun.* **2011**, *47*, 10936.
- [46] R. Janot, D. Guerard, *Carbon* **2002**, *40*, 2887.
- [47] C. Damm, T. J. Nacken, W. Peukert, *Carbon* **2015**, *81*, 284.
- [48] I. Y. Jeon, Y. R. Shin, G. J. Sohn, H. J. Choi, S. Y. Bae, J. Mahmood, S. M. Jung, J. M. Seo, M. J. Kim, D. W. Chang, L. M. Dai, J. B. Baek, *Proc. Natl. Acad. Sci. U.S.A.* **2012**, *109*, 5588.
- [49] I. Y. Jeon, H. J. Choi, S. M. Jung, J. M. Seo, M. J. Kim, L. M. Dai, J. B. Baek, *J. Am. Chem. Soc.* **2013**, *135*, 1386.
- [50] W. Qian, R. Hao, Y. L. Hou, Y. Tian, C. M. Shen, H. J. Gao, X. L. Liang, *Nano Res.* **2009**, *2*, 706.
- [51] Z. H. Tang, J. Zhuang, X. Wang, *Langmuir* **2010**, *26*, 9045.
- [52] A. M. Abdelkader, A. J. Cooper, R. A. W. Dryfe, I. A. Kinloch, *Nanoscale* **2015**, *7*, 6944.

- [53] K. Parvez, Z. S. Wu, R. J. Li, X. J. Liu, R. Graf, X. L. Feng, K. Müllen, *J. Am. Chem. Soc.* **2014**, *136*, 6083.
- [54] G. X. Wang, B. Wang, J. Park, Y. Wang, B. Sun, J. Yao, *Carbon* **2009**, *47*, 3242.
- [55] K. Parvez, R. J. Li, S. R. Puniredd, Y. Hernandez, F. Hinkel, S. H. Wang, X. L. Feng, K. Müllen, *Acs Nano* **2013**, *7*, 3598.
- [56] J. M. Munuera, J. I. Paredes, S. Villar-Rodil, M. Ayan-Varela, A. Pagan, S. D. Aznar-Cervantes, J. L. Cenis, A. Martinez-Alonso, J. M. D. Tascon, *Carbon* **2015**, *94*, 729.
- [57] K. R. Paton, E. Varrla, C. Backes, R. J. Smith, U. Khan, A. O'Neill, C. Boland, M. Lotya, O. M. Istrate, P. King, T. Higgins, S. Barwich, P. May, P. Puczarski, I. Ahmed, M. Moebius, H. Pettersson, E. Long, J. Coelho, S. E. O'Brien, E. K. McGuire, B. M. Sanchez, G. S. Duesberg, N. McEvoy, T. J. Pennycook, C. Downing, A. Crossley, V. Nicolosi, J. N. Coleman, *Nat. Mater.* **2014**, *13*, 624.
- [58] E. Varrla, K. R. Paton, C. Backes, A. Harvey, R. J. Smith, J. McCauley, J. N. Coleman, *Nanoscale* **2014**, *6*, 11810.
- [59] J. N. Coleman, M. Lotya, A. O'Neill, S. D. Bergin, P. J. King, U. Khan, K. Young, A. Gaucher, S. De, R. J. Smith, I. V. Shvets, S. K. Arora, G. Stanton, H. Y. Kim, K. Lee, G. T. Kim, G. S. Duesberg, T. Hallam, J. J. Boland, J. J. Wang, J. F. Donegan, J. C. Grunlan, G. Moriarty, A. Shmeliov, R. J. Nicholls, J. M. Perkins, E. M. Grieveson, K. Theuwissen, D. W. McComb, P. D. Nellist, V. Nicolosi, *Science* **2011**, *331*, 568.
- [60] V. Nicolosi, M. Chhowalla, M. G. Kanatzidis, M. S. Strano, J. N. Coleman, *Science* **2013**, *340*, 1420.
- [61] A. Ciesielski, P. Samorì, *Chem. Soc. Rev.* **2014**, *43*, 381.
- [62] K. Parvez, S. Yang, X. L. Feng, K. Müllen, *Synt. Met.* **2015**, doi:10.1016/j.synthmet.2015.07.014.
- [63] Y. Hernandez, V. Nicolosi, M. Lotya, F. M. Blighe, Z. Sun, S. De, I. T. McGovern, B. Holland, M. Byrne, Y. K. Gun'Ko, J. J. Boland, P. Niraj, G. Duesberg, S. Krishnamurthy, R. Goodhue, J. Hutchison, V. Scardaci, A. C. Ferrari, J. N. Coleman, *Nat. Nanotechnol.* **2008**, *3*, 563.
- [64] Y. L. Zhong, Z. M. Tian, G. P. Simon, D. Li, *Mater. Today* **2015**, *18*, 73.
- [65] A. Schlierf, P. Samorì, V. Palermo, *J. Mat. Chem. C* **2014**, *2*, 3129.
- [66] N. Behabtu, J. R. Lomeda, M. J. Green, A. L. Higginbotham, A. Sinitskii, D. V. Kosynkin, D. Tsentelovich, A. N. G. Parra-Vasquez, J. Schmidt, E. Kesselman, Y. Cohen, Y. Talmon, J. M. Tour, M. Pasquali, *Nat. Nanotechnol.* **2010**, *5*, 406.
- [67] J. N. Coleman, *Adv. Func. Mater.* **2009**, *19*, 3680.
- [68] J. N. Coleman, *Acc. Chem. Res.* **2013**, *46*, 14.
- [69] O. M. Marago, F. Bonaccorso, R. Saija, G. Privitera, P. G. Gucciardi, M. A. Iati, G. Calogero, P. H. Jones, F. Borghese, P. Denti, V. Nicolosi, A. C. Ferrari, *Acs Nano* **2010**, *4*, 7515.
- [70] F. Torrisi, T. Hasan, W. P. Wu, Z. P. Sun, A. Lombardo, T. S. Kulmala, G. W. Hsieh, S. J. Jung, F. Bonaccorso, P. J. Paul, D. P. Chu, A. C. Ferrari, *Acs Nano* **2012**, *6*, 2992.
- [71] A. Capasso, A. E. Del Rio Castillo, H. Sun, A. Ansaldò, V. Pellegrini, F. Bonaccorso, *Solid State Commun.* **2015**, doi:10.1016/j.ssc.2015.08.011.
- [72] F. Torrisi, J. N. Coleman, *Nat. Nanotechnol.* **2014**, *9*, 738.
- [73] B. C. Brodie, *Philos. Trans. R. Soc. London* **1859**, *149*, 249.
- [74] L. Staudenmaier, *Ber. Dtsch. Chem. Ges.* **1898**, *31*, 1481.
- [75] W. S. Hummers, R. E. Offeman, *J. Am. Chem. Soc.* **1958**, *80*, 1339.
- [76] S. Stankovich, D. A. Dikin, R. D. Piner, K. A. Kohlhaas, A. Kleinhammes, Y. Jia, Y. Wu, S. T. Nguyen, R. S. Ruoff, *Carbon* **2007**, *45*, 1558.
- [77] G. Eda, G. Fanchini, M. Chhowalla, *Nat. Nanotechnol.* **2008**, *3*, 270.
- [78] C. Gomez-Navarro, R. T. Weitz, A. M. Bittner, M. Scolari, A. Mews, M. Burghard, K. Kern, *Nano Lett.* **2007**, *7*, 3499.

- [79] K. N. Kudin, B. Ozbas, H. C. Schniepp, R. K. Prud'homme, I. A. Aksay, R. Car, *Nano Lett.* **2008**, *8*, 36.
- [80] D. Yang, A. Velamakanni, G. Bozoklu, S. Park, M. Stoller, R. D. Piner, S. Stankovich, I. Jung, D. A. Field, C. A. Ventrice, R. S. Ruoff, *Carbon* **2009**, *47*, 145.
- [81] X. Huang, X. Y. Qi, F. Boey, H. Zhang, *Chem. Soc. Rev.* **2012**, *41*, 666.
- [82] X. Huang, Z. Y. Yin, S. X. Wu, X. Y. Qi, Q. Y. He, Q. C. Zhang, Q. Y. Yan, F. Boey, H. Zhang, *Small* **2011**, *7*, 1876.
- [83] T. F. Yeh, J. M. Syu, C. Cheng, T. H. Chang, H. S. Teng, *Adv. Func. Mater.* **2010**, *20*, 2255.
- [84] J. Pyun, *Angew. Chem. Int. Ed.* **2011**, *50*, 46.
- [85] I. V. Lightcap, P. V. Kamat, *Acc. Chem. Res.* **2013**, *46*, 2235.
- [86] C. Chung, Y. K. Kim, D. Shin, S. R. Ryoo, B. H. Hong, D. H. Min, *Acc. Chem. Res.* **2013**, *46*, 2211.
- [87] V. Georgakilas, J. A. Perman, J. Tucek, R. Zboril, *Chem. Rev.* **2015**, *115*, 4744.
- [88] D. C. Wei, Y. Q. Liu, Y. Wang, H. L. Zhang, L. P. Huang, G. Yu, *Nano Lett.* **2009**, *9*, 1752.
- [89] T. B. Martins, R. H. Miwa, A. J. R. da Silva, A. Fazzio, *Phys Rev Lett* **2007**, *98*, 196803.
- [90] X. R. Wang, X. L. Li, L. Zhang, Y. Yoon, P. K. Weber, H. L. Wang, J. Guo, H. J. Dai, *Science* **2009**, *324*, 768.
- [91] J. Choi, K. J. Kim, B. Kim, H. Lee, S. Kim, *J. Phys. Chem. C* **2009**, *113*, 9433.
- [92] J. Choi, H. Lee, K. J. Kim, B. Kim, S. Kim, *J. Phys. Chem. Lett.* **2010**, *1*, 505.
- [93] Z. X. Zhang, H. L. Huang, X. M. Yang, L. Zang, *J. Phys. Chem. Lett.* **2011**, *2*, 2897.
- [94] K. S. Mali, J. Greenwood, J. Adisojoso, R. Phillipson, S. De Feyter, *Nanoscale* **2015**, *7*, 1566.
- [95] J. M. MacLeod, F. Rosei, *Small* **2014**, *10*, 1038.
- [96] W. Feng, W. Luo, Y. Y. Feng, *Nanoscale* **2012**, *4*, 6118.
- [97] J. Israelachvili, *Intermolecular & Surface Forces*, Academic Press, London, **1992**.
- [98] H. Margenau, *Rev. Mod. Phys.* **1939**, *11*, 1.
- [99] J. P. Rabe, S. Buchholz, *Science* **1991**, *253*, 424.
- [100] P. Samori, A. Fechtenkötter, F. Jäckel, T. Böhme, K. Müllen, J. P. Rabe, *J. Am. Chem. Soc.* **2001**, *123*, 11462.
- [101] A. J. Gellman, K. R. Paserba, *J. Phys. Chem. B* **2002**, *106*, 13231.
- [102] J. Björk, F. Hanke, C.-A. Palma, P. Samori, M. Cecchini, M. Persson, *J. Phys. Chem. Lett.* **2010**, *1*, 3407.
- [103] R. Zacharia, H. Ulbricht, T. Hertel, *Phys. Rev. B* **2004**, *69*, 155406.
- [104] M. Kastler, W. Pisula, D. Wasserfallen, T. Pakula, K. Müllen, *J. Am. Chem. Soc.* **2005**, *127*, 4286.
- [105] S. D. Bergin, V. Nicolosi, P. V. Streich, S. Giordani, Z. Y. Sun, A. H. Windle, P. Ryan, N. P. P. Niraj, Z. T. T. Wang, L. Carpenter, W. J. Blau, J. J. Boland, J. P. Hamilton, J. N. Coleman, *Adv. Mater.* **2008**, *20*, 1876.
- [106] U. Khan, A. O'Neill, M. Lotya, S. De, J. N. Coleman, *Small* **2010**, *6*, 864.
- [107] U. Khan, A. O'Neill, H. Porwal, P. May, K. Nawaz, J. N. Coleman, *Carbon* **2012**, *50*, 470.
- [108] A. O'Neill, U. Khan, P. N. Nirmalraj, J. Boland, J. N. Coleman, *J. Phys. Chem. C* **2011**, *115*, 5422.
- [109] X. Y. Zhang, A. C. Coleman, N. Katsonis, W. R. Browne, B. J. van Wees, B. L. Feringa, *Chem. Commun.* **2010**, *46*, 7539.
- [110] T. J. Mason, J. Phillip, *Applied Sonochemistry*, Wiley-VCH Weinheim, **2002**.
- [111] G. Cravotto, P. Cintas, *Chem. Eur. J.* **2010**, *16*, 5246.
- [112] K. R. Paserba, A. J. Gellman, *Phys Rev Lett* **2001**, *86*, 4338

- [113] S. L. Tait, Z. Dohnálek, C. T. Campbell, B. D. Kay, *J. Chem. Phys.* **2006**, *125*, 234308.
- [114] K. R. Paserba, A. J. Gellman, *J. Chem. Phys.* **2001**, *115*, 6737.
- [115] D. Bonifazi, S. Mohnani, A. Llanes-Pallas, *Chem. Eur. J.* **2009**, *15*, 7004.
- [116] A. Ciesielski, C.-A. Palma, M. Bonini, P. Samorì, *Adv. Mater.* **2010**, *22*, 3506.
- [117] A. Ciesielski, P. Samorì, *Nanoscale* **2011**, *3*, 1397.
- [118] S. De Feyter, F. C. De Schryver, *Chem. Soc. Rev.* **2003**, *32*, 139.
- [119] J. M. MacLeod, F. Rosei, *Small* **2014**, *10*, 1038.
- [120] K. S. Mali, J. Greenwood, J. Adisojoso, R. Phillipson, S. De Feyter, *Nanoscale* **2015**, *7*, 1566.
- [121] P. Lauffer, K. V. Emtsev, R. Graupner, T. Seyller, L. Ley, *Phys. Status Solidi (B)* **2008**, *245*, 2064.
- [122] Q. H. Wang, M. C. Hersam, *Nat. Chem.* **2009**, *1*, 206.
- [123] H. Huang, S. Chen, X. Y. Gao, W. Chen, A. T. S. Wee, *Acs Nano* **2009**, *3*, 3431.
- [124] G. Binnig, H. Rohrer, C. Gerber, E. Weibel, *Phys Rev Lett* **1982**, *49*, 57.
- [125] H. Rohrer, *Proc. Natl. Acad. Sci. U.S.A* **1987**, *84*, 4666.
- [126] F. Ciccoira, C. Santato, F. Rosei, in *Top. Curr. Chem.*, Springer, **2008**, pp. 203.
- [127] L. Kampschulte, T. L. Werblowsky, R. S. K. Kishore, M. Schmittel, W. M. Heckl, M. Lackinger, *J. Am. Chem. Soc.* **2008**, *130*, 8502.
- [128] T. Kudernac, S. B. Lei, J. A. A. W. Elemans, S. De Feyter, *Chem. Soc. Rev.* **2009**, *38*, 402.
- [129] J. M. MacLeod, O. Ivasenko, D. F. Perepichka, F. Rosei, *Nanotechnology* **2007**, *18*, 3347.
- [130] A. Ciesielski, M. El Garah, S. Haar, P. Kovaricek, J. M. Lehn, P. Samorì, *Nat Chem* **2014**, *6*, 1017.
- [131] X. Q. Tian, J. B. Xu, X. M. Wang, *J Phys Chem C* **2010**, *114*, 20917.
- [132] M. Meissner, M. Gruenewald, F. Sojka, C. Udhardt, R. Forker, T. Fritz, *Surf. Sci.* **2012**, *606*, 1709.
- [133] J. H. Mao, H. G. Zhang, Y. H. Jiang, Y. Pan, M. Gao, W. D. Xiao, H. J. Gao, *J Am Chem Soc* **2009**, *131*, 14136.
- [134] H. G. Zhang, J. T. Sun, T. Low, L. Z. Zhang, Y. Pan, Q. Liu, J. H. Mao, H. T. Zhou, H. M. Guo, S. X. Du, F. Guinea, H. J. Gao, *Phys Rev B* **2011**, *84*, 245436.
- [135] K. Yang, W. D. Xiao, Y. H. Jiang, H. G. Zhang, L. W. Liu, J. H. Mao, H. T. Zhou, S. X. Du, H. J. Gao, *J Phys Chem C* **2012**, *116*, 14052.
- [136] Y. L. Wang, J. Ren, C. L. Song, Y. P. Jiang, L. L. Wang, K. He, X. Chen, J. F. Jia, S. Meng, E. Kaxiras, Q. K. Xue, X. C. Ma, *Phys Rev B* **2010**, *82*, 245420.
- [137] M. Scardamaglia, S. Lisi, S. Lizzit, A. Baraldi, R. Larciprete, C. Mariani, M. G. Betti, *J Phys Chem C* **2013**, *117*, 3019.
- [138] S. K. Haïmäläinen, M. Stepanova, R. Drost, P. Liljeroth, J. Lahtinen, J. Sainio, *J Phys Chem C* **2012**, *116*, 20433.
- [139] W. D. Dou, S. P. Huang, R. Q. Zhang, C. S. Lee, *J. Chem. Phys.* **2011**, *134*, 094705.
- [140] H. Y. Mao, R. Wang, Y. Wang, T. C. Niu, J. Q. Zhong, M. Y. Huang, D. C. Qi, K. P. Loh, A. T. S. Wee, W. Chen, *Appl Phys Lett* **2011**, *99*, 093301.
- [141] K. Xiao, W. Deng, J. K. Keum, M. Yoon, I. V. Vlassiuk, K. W. Clark, A. P. Li, I. I. Kravchenko, G. Gu, E. A. Payzant, B. G. Sumpter, S. C. Smith, J. F. Browning, D. B. Geohegan, *J Am Chem Soc* **2013**, *135*, 3680.
- [142] J. Wintterlin, M. L. Bocquet, *Surf. Sci.* **2009**, *603*, 1841.
- [143] H. T. Zhou, J. H. Mao, G. Li, Y. L. Wang, X. L. Feng, S. X. Du, K. Müllen, H. J. Gao, *Appl Phys Lett* **2011**, *99*, 153101.
- [144] G. Li, H. T. Zhou, L. D. Pan, Y. Zhang, J. H. Mao, Q. Zou, H. M. Guo, Y. L. Wang, S. X. Du, H. J. Gao, *Appl Phys Lett* **2012**, *100*, 013304.

- [145] J. Lu, P. S. E. Yeo, Y. Zheng, Z. Y. Yang, Q. L. Bao, C. K. Gan, K. P. Loh, *Acs Nano* **2012**, *6*, 944.
- [146] J. Cho, J. Smerdon, L. Gao, O. Suzer, J. R. Guest, N. P. Guisinger, *Nano Lett* **2012**, *12*, 3018.
- [147] M. Roos, B. Uhl, D. Künzel, H. E. Hoster, A. Gross, R. J. Behm, *Beilstein J. Nanotechnol.* **2011**, *2*, 365.
- [148] C. Meier, M. Roos, D. Kunzel, A. Breitruck, H. E. Hoster, K. Landfester, A. Gross, R. J. Behm, U. Ziener, *J Phys Chem C* **2010**, *114*, 1268.
- [149] B. Li, K. Tahara, J. Adisojoso, W. Vanderlinden, K. S. Mali, S. De Gendt, Y. Tobe, S. De Feyter, *Acs Nano* **2013**, *7*, 10764.
- [150] B. Li, A. V. Klekachev, M. Cantoro, C. Huyghebaert, A. Stesmans, I. Asselberghs, S. De Gendt, S. De Feyter, *Nanoscale* **2013**, *5*, 9640.
- [151] M. C. Prado, R. Nascimento, L. G. Moura, M. J. S. Matos, M. S. C. Mazzoni, L. G. Cancado, H. Chacham, B. R. A. Neves, *Acs Nano* **2011**, *5*, 394.
- [152] X. Y. Zhang, E. H. Huisman, M. Gurram, W. R. Browne, B. J. van Wees, B. L. Feringa, *Small* **2014**, *10*, 1735.
- [153] Y. Y. Shao, J. Wang, H. Wu, J. Liu, I. A. Aksay, Y. H. Lin, *Electroanal* **2010**, *22*, 1027.
- [154] T. Kuila, S. Bose, P. Khanra, A. K. Mishra, N. H. Kim, J. H. Lee, *Biosens. Bioelectron.* **2011**, *26*, 4637.
- [155] S. J. Sheng, S. Liu, L. Y. Zhang, G. Chen, *Chem. Asian J.* **2013**, *8*, 191.
- [156] M. Pumera, A. Ambrosi, A. Bonanni, E. L. K. Chng, H. L. Poh, *Trends Anal. Chem.* **2010**, *29*, 954.
- [157] A. Ambrosi, T. Sasaki, M. Pumera, *Chem. Asian J.* **2010**, *5*, 266.
- [158] G. Cunningham, M. Lotya, C. S. Cucinotta, S. Sanvito, S. D. Bergin, R. Menzel, M. S. P. Shaffer, J. N. Coleman, *Acs Nano* **2012**, *6*, 3468.
- [159] K. Lee, H. Y. Kim, M. Lotya, J. N. Coleman, G. T. Kim, G. S. Duesberg, *Adv. Mater.* **2011**, *23*, 4178.
- [160] D. Hanlon, C. Backes, E. Doherty, C. S. Cucinotta, N. C. Berner, C. Boland, K. Lee, A. Harvey, P. Lynch, Z. Gholamvand, S. Zhang, K. Wang, G. Moynihan, A. Pokle, Q. M. Ramasse, N. McEvoy, W. J. Blau, J. Wang, G. Abellan, F. Hauke, A. Hirsch, S. Sanvito, D. D. O'Regan, G. S. Duesberg, V. Nicolosi, J. N. Coleman, *Nat Commun* **2015**, *6*, 8563.
- [161] R. Bari, D. Parviz, F. Khabaz, C. D. Klaassen, S. D. Metzler, M. J. Hansen, R. Khare, M. J. Green, *Phys. Chem. Chem. Phys.* **2015**, *17*, 9383.
- [162] H. M. Solomon, B. A. Burgess, G. L. Kennedy, R. E. Staples, *Drug Chem. Toxicol.* **1995**, *18*, 271.
- [163] G. L. Kennedy, H. Sherman, *Drug Chem. Toxicol.* **1986**, *9*, 147.
- [164] A. B. Bourlinos, V. Georgakilas, R. Zboril, T. A. Steriotis, A. K. Stubos, *Small* **2009**, *5*, 1841.
- [165] A. J. Oyer, J. M. Y. Carrillo, C. C. Hire, H. C. Schniepp, A. D. Asandei, A. V. Dobrynin, D. H. Adamson, *J. Am. Chem. Soc.* **2012**, *134*, 5018.
- [166] Z. Y. Sun, X. Huang, F. Liu, X. N. Yang, C. Rösler, R. A. Fischer, M. Muhler, W. Schuhmann, *Chem. Commun.* **2014**, *50*, 10382.
- [167] S. Ravula, S. N. Baker, G. Kamath, G. A. Baker, *Nanoscale* **2015**, *7*, 4338.
- [168] T. Fukushima, A. Kosaka, Y. Ishimura, T. Yamamoto, T. Takigawa, N. Ishii, T. Aida, *Science* **2003**, *300*, 2072.
- [169] X. S. Zhou, T. B. Wu, K. L. Ding, B. J. Hu, M. Q. Hou, B. X. Han, *Chem. Commun.* **2010**, *46*, 386.
- [170] X. Q. Wang, P. F. Fulvio, G. A. Baker, G. M. Veith, R. R. Unocic, S. M. Mahurin, M. F. Chi, S. Dai, *Chem. Commun.* **2010**, *46*, 4487.

- [171] D. Nuvoli, L. Valentini, V. Alzari, S. Scognamillo, S. B. Bon, M. Piccinini, J. Illescas, A. Mariani, *J. Mater. Chem.* **2011**, *21*, 3428.
- [172] R. Bari, G. Tamas, F. Irin, A. J. A. Aquino, M. J. Green, E. L. Quitevis, *Colloids Surf., A* **2014**, *463*, 63.
- [173] A. C. Ferrari, J. C. Meyer, V. Scardaci, C. Casiraghi, M. Lazzeri, F. Mauri, S. Piscanec, D. Jiang, K. S. Novoselov, S. Roth, A. K. Geim, *Phys Rev Lett* **2006**, *97*, 187401.
- [174] C. Valles, C. Drummond, H. Saadaoui, C. A. Furtado, M. He, O. Roubeau, L. Ortolani, M. Monthieux, A. Penicaud, *J. Am. Chem. Soc.* **2008**, *130*, 15802.
- [175] A. C. Ferrari, D. M. Basko, *Nat. Nanotechnol.* **2013**, *8*, 235.
- [176] C. Casiraghi, in *Spectroscopic Properties of Inorganic and Organometallic Compounds: Techniques, Materials and Applications, Volume 43, Vol. 43* (Eds.: J. Yarwood, R. Douthwaite, S. Duckett), The Royal Society of Chemistry, Cambridge, UK, **2012**, pp. 29.
- [177] C. F. Chen, C. H. Park, B. W. Boudouris, J. Horng, B. S. Geng, C. Girit, A. Zettl, M. F. Crommie, R. A. Segalman, S. G. Louie, F. Wang, *Nature* **2011**, *471*, 617.
- [178] A. Das, B. Chakraborty, S. Piscanec, S. Pisana, A. K. Sood, A. C. Ferrari, *Phys. Rev. B* **2009**, *79*, 155417.
- [179] A. Das, S. Pisana, B. Chakraborty, S. Piscanec, S. K. Saha, U. V. Waghmare, K. S. Novoselov, H. R. Krishnamurthy, A. K. Geim, A. C. Ferrari, A. K. Sood, *Nat. Nanotechnol.* **2008**, *3*, 210.
- [180] M. Kalbac, A. Reina-Cecco, H. Farhat, J. Kong, L. Kavan, M. S. Dresselhaus, *Acs Nano* **2010**, *4*, 6055.
- [181] J. Yan, Y. B. Zhang, P. Kim, A. Pinczuk, *Phys Rev Lett* **2007**, *98*, 166802.
- [182] W. J. Zhao, P. H. Tan, J. Liu, A. C. Ferrari, *J. Am. Chem. Soc.* **2011**, *133*, 5941.
- [183] D. M. Basko, *Phys. Rev. B* **2009**, *79*, 205428.
- [184] C. Casiraghi, A. Hartschuh, H. Qian, S. Piscanec, C. Georgi, A. Fasoli, K. S. Novoselov, D. M. Basko, A. C. Ferrari, *Nano Lett.* **2009**, *9*, 1433.
- [185] C. X. Cong, T. Yu, H. M. Wang, *Acs Nano* **2010**, *4*, 3175.
- [186] A. K. Gupta, T. J. Russin, H. R. Gutierrez, P. C. Eklund, *Acs Nano* **2009**, *3*, 45.
- [187] Y. M. You, Z. H. Ni, T. Yu, Z. X. Shen, *Appl. Phys. Lett.* **2008**, *93*, 163112.
- [188] J. H. Chen, W. G. Cullen, C. Jang, M. S. Fuhrer, E. D. Williams, *Phys Rev Lett* **2009**, *102*, 236805.
- [189] Z. H. Ni, L. A. Ponomarenko, R. R. Nair, R. Yang, S. Anissimova, I. V. Grigorieva, F. Schedin, P. Blake, Z. X. Shen, E. H. Hill, K. S. Novoselov, A. K. Geim, *Nano Lett.* **2010**, *10*, 3868.
- [190] T. Gokus, R. R. Nair, A. Bonetti, M. Bohmler, A. Lombardo, K. S. Novoselov, A. K. Geim, A. C. Ferrari, A. Hartschuh, *Acs Nano* **2009**, *3*, 3963.
- [191] J. N. Israelachvili, *Intermolecular and surface forces*, third ed., Academic Press, Waltham, USA, **2011**.
- [192] S. R. Wang, Y. Zhang, N. Abidi, L. Cabrales, *Langmuir* **2009**, *25*, 11078.
- [193] A. Bianco, *Angew. Chem. Int. Ed.* **2013**, *52*, 4986.
- [194] R. Kurapati, J. Russier, M. A. Squillaci, E. Treossi, C. Menard-Moyon, A. E. Del Rio-Castillo, E. Vazquez, P. Samorì, V. Palermo, A. Bianco, *Small* **2015**, *11*, 3985.
- [195] M. Lotya, Y. Hernandez, P. J. King, R. J. Smith, V. Nicolosi, L. S. Karlsson, F. M. Blighe, S. De, Z. M. Wang, I. T. McGovern, G. S. Duesberg, J. N. Coleman, *J. Am. Chem. Soc.* **2009**, *131*, 3611.
- [196] M. Lotya, P. J. King, U. Khan, S. De, J. N. Coleman, *Acs Nano* **2010**, *4*, 3155.
- [197] T. Skaltsas, N. Karousis, H. Yan, C.-R. Wang, S. Pispas, N. Tagmatarchis, *J. Mater. Chem.* **2012**, 21507.
- [198] F. Liu, J. Y. Choi, T. S. Seo, *Chem. Commun.* **2010**, *46*, 2844.

- [199] S. Bose, T. Kuila, A. K. Mishra, N. H. Kim, J. H. Lee, *Nanotechnology* **2011**, *22*, 1.
- [200] J. M. Englert, J. Rohrl, C. D. Schmidt, R. Graupner, M. Hundhausen, F. Hauke, A. Hirsch, *Adv. Mater.* **2009**, *21*, 4265.
- [201] A. Ghosh, K. V. Rao, S. J. George, C. N. R. Rao, *Chem. Eur. J.* **2010**, *16*, 2700.
- [202] Q. Su, S. P. Pang, V. Alijani, C. Li, X. L. Feng, K. Müllen, *Adv. Mater.* **2009**, *21*, 3191.
- [203] H. Zhang, J. Q. Wen, X. P. Meng, Y. D. Yao, G. F. Yin, X. M. Liao, Z. B. Huang, *Chem. Lett.* **2012**, *41*, 747.
- [204] X. L. Feng, V. Marcon, W. Pisula, M. R. Hansen, J. Kirkpatrick, F. Grozema, D. Andrienko, K. Kremer, K. Müllen, *Nat. Mater.* **2009**, *8*, 421.
- [205] C. Li, M. Y. Liu, N. G. Pschirer, M. Baumgarten, K. Müllen, *Chem. Rev.* **2010**, *110*, 6817.
- [206] R. Rieger, K. Müllen, *J. Phys. Org. Chem.* **2010**, *23*, 315.
- [207] B. Schmaltz, T. Weil, K. Müllen, *Adv. Mater.* **2009**, *21*, 1067.
- [208] Z. J. Chen, A. Lohr, C. R. Saha-Moller, F. Wurthner, *Chem. Soc. Rev.* **2009**, *38*, 564.
- [209] T. Fujigaya, N. Nakashima, *Polym. J.* **2008**, *40*, 577.
- [210] X. Dong, Y. Shi, Y. Zhao, D. Chen, J. Ye, Y. Yao, F. Gao, Z. Ni, T. Yu, Z. Shen, *Phys Rev Lett* **2009**, *102*, 135501.
- [211] J.-H. Jang, D. Rangappa, Y.-U. Kwon, I. Honma, *J. Mater. Chem.* **2010**, *21*, 3462.
- [212] D. W. Lee, T. Kim, M. Lee, *Chem. Commun.* **2011**, *47*, 8259.
- [213] A. Schlierf, H. Yang, E. Gebremedhn, E. Treossi, L. Ortolani, L. Chen, A. Minoia, V. Morandi, P. Samori, C. Casiraghi, D. Beljonne, V. Palermo, *Nanoscale* **2013**, *5*, 4205.
- [214] H. Yang, Y. Hernandez, A. Schlierf, A. Felten, A. Eckmann, S. Johal, P. Louette, J. J. Pireaux, X. Feng, K. Muellen, V. Palermo, C. Casiraghi, *Carbon* **2013**, *53*, 357.
- [215] D. Parviz, S. Das, H. S. T. Ahmed, F. Irin, S. Bhattacharia, M. J. Green, *Acs Nano* **2012**, *6*, 8857.
- [216] F. Zhang, X. J. Chen, R. A. Boulos, F. M. Yasin, H. B. Lu, C. Raston, H. B. Zhang, *Chem. Commun.* **2013**, *49*, 4845.
- [217] H. W. Shim, K.-J. Ahn, K. Im, S. Noh, M.-S. Kim, Y. Lee, H. Choi, H. Yoon, *Macromolecules* **2015**, *48*, 6628.
- [218] M. Zhang, R. R. Parajuli, D. Mastrogiovanni, B. Dai, P. Lo, W. Cheung, R. Brukh, P. L. Chiu, T. Zhou, Z. F. Liu, E. Garfunkel, H. X. He, *Small* **2010**, *6*, 1100.
- [219] Y. X. Xu, H. Bai, G. W. Lu, C. Li, G. Q. Shi, *J. Am. Chem. Soc.* **2008**, *130*, 5856.
- [220] L. Zhang, Z. J. Zhang, C. Z. He, L. M. Dai, J. Liu, L. X. Wang, *Acs Nano* **2014**, *8*, 6663.
- [221] N. V. Kozhemyakina, J. M. Englert, G. A. Yang, E. Spiecker, C. D. Schmidt, F. Hauke, A. Hirsch, *Adv. Mater.* **2010**, *22*, 5483.
- [222] S. Sampath, A. N. Basuray, K. J. Hartlieb, T. Aytun, S. I. Stupp, J. F. Stoddart, *Adv. Mater.* **2013**, *25*, 2740.
- [223] S. Ahadian, M. Estili, V. J. Surya, J. Ramon-Azcon, X. B. Liang, H. Shiku, M. Ramalingam, T. Matsue, Y. Sakka, H. Bae, K. Nakajima, Y. Kawazoe, A. Khademhosseini, *Nanoscale* **2015**, *7*, 6436.
- [224] A. B. Bourlinos, V. Georgakilas, R. Zboril, T. A. Steriotis, A. K. Stubos, C. Trapalis, *Solid State Commun.* **2009**, *149*, 2172.
- [225] V. Chabot, B. Kim, B. Sloper, C. Tzoganakis, A. P. Yu, *Sci. Rep.* **2013**, *3*.
- [226] J. C. Fan, Z. X. Shi, Y. Ge, J. L. Wang, Y. Wang, J. Yin, *J. Mater. Chem.* **2012**, *22*, 13764.
- [227] Y. Ge, J. L. Wang, Z. X. Shi, J. Yin, *J. Mater. Chem.* **2012**, *22*, 17619.
- [228] L. Guardia, M. J. Fernandez-Merino, J. I. Paredes, P. Solis-Fernandez, S. Villar-Rodil, A. Martinez-Alonso, J. M. D. Tascon, *Carbon* **2011**, *49*, 1653.
- [229] Y. T. Liang, M. C. Hersam, *J. Am. Chem. Soc.* **2010**, *132*, 17661.

- [230] W. S. Liu, R. Zhou, D. Zhou, G. G. Ding, J. M. Soah, C. Y. Yue, X. H. Lu, *Carbon* **2015**, *83*, 188.
- [231] M. T. Popescu, D. Tasis, C. Tsitsilianis, *ACS Macro Lett.* **2014**, *3*, 981.
- [232] I. U. Unalan, C. Y. Wan, S. Trabattoni, L. Piergiovanni, S. Farris, *Rsc Adv.* **2015**, *5*, 26482.
- [233] P. May, U. Khan, J. M. Hughes, J. N. Coleman, *J. Phys. Chem. C* **2012**, *116*, 11393.
- [234] X. Yang, F. Zhang, L. Zhang, T. F. Zhang, Y. Huang, Y. S. Chen, *Adv. Func. Mater.* **2013**, *23*, 3353.
- [235] M. Ayan-Varela, J. I. Paredes, L. Guardia, S. Villar-Rodil, J. M. Munuera, M. Diaz-Gonzalez, C. Fernandez-Sanchez, A. Martinez-Alonso, J. M. D. Tascon, *ACS Appl. Mater. Interfaces* **2015**, *7*, 10293.
- [236] I. W. P. Chen, Y. S. Chen, N. J. Kao, C. W. Wu, Y. W. Zhang, H. T. Li, *Carbon* **2015**, *90*, 16.
- [237] I. W. P. Chen, C.-Y. Huang, S.-H. S. Jhou, Y.-W. Zhang, *Sci. Rep.* **2014**, *4*, 3928.
- [238] S. De, P. J. King, M. Lotya, A. O'Neill, E. M. Doherty, Y. Hernandez, G. S. Duesberg, J. N. Coleman, *Small* **2010**, *6*, 458.
- [239] R. Hao, W. Qian, L. H. Zhang, Y. L. Hou, *Chem. Commun.* **2008**, 6576.
- [240] P. He, C. Zhou, S. Y. Tian, J. Sun, S. W. Yang, G. Q. Ding, X. M. Xie, M. H. Jiang, *Chem. Commun.* **2015**, *51*, 4651.
- [241] W. Lee, D. W. Lee, M. Lee, J. I. Hong, *Chem. Commun.* **2014**, *50*, 14851.
- [242] V. M. Samoilov, E. A. Danilov, A. V. Nikolaeva, G. A. Yerpuleva, N. N. Trofimova, S. S. Abramchuk, K. V. Ponkratov, *Carbon* **2015**, *84*, 38.
- [243] A. Schlierf, K. Cha, M. G. Schwab, P. Samorì, V. Palermo, *2d Materials* **2014**, *1*, 035006.
- [244] M. H. Wahid, U. H. Stroehrer, E. Eroglu, X. J. Chen, K. Vimalanathan, C. L. Raston, R. A. Boulos, *J. Colloid Interface Sci.* **2015**, *443*, 88.
- [245] W. J. Hyun, E. B. Secor, M. C. Hersam, C. D. Frisbie, L. F. Francis, *Adv. Mater.* **2015**, *27*, 109.
- [246] L. L. Chua, J. Zaumseil, J. F. Chang, E. C. W. Ou, P. K. H. Ho, H. Sirringhaus, R. H. Friend, *Nature* **2005**, *434*, 194.
- [247] A. Ciesielski, S. Haar, M. El Gemayel, H. Yang, J. Clough, G. Melinte, N. Gobbi, E. Orgiu, M. V. Nardi, G. Ligorio, V. Palermo, N. Koch, O. Ersen, C. Casiraghi, P. Samorì, *Angew. Chem. Int. Ed.* **2014**, *53*, 10355.
- [248] J. Geng, B. S. Kong, S. B. Yang, H. T. Jung, *Chem. Commun.* **2010**, *46*, 5091.
- [249] S. Haar, A. Ciesielski, J. Clough, H. Yang, R. Mazzaro, F. Richard, S. Conti, N. Merstorf, M. Cecchini, V. Morandi, C. Casiraghi, P. Samorì, *Small* **2015**, *11*, 1691.
- [250] X. Li, G. Zhang, X. Bai, X. Sun, X. Wang, E. Wang, H. Dai, *Nat. Nanotechnol.* **2008**, *3*, 538.
- [251] S. R. Pathipati, E. Pavlica, A. Schlierf, M. El Gemayel, P. Samorì, V. Palermo, G. Bratina, *J. Phys. Chem. C* **2014**, *118*, 24819.
- [252] S. Vadukumpully, J. Paul, S. Valiyaveetil, *Carbon* **2009**, *47*, 3288.
- [253] L. Xu, J.-W. McGraw, F. Gao, M. Grundy, Z. Ye, Z. Gu, J. L. Shepherd, *J. Phys. Chem. C* **2013**, *117*, 10730.
- [254] T. Hasobe, H. Imahori, P. V. Kamat, T. K. Ahn, S. K. Kim, D. Kim, A. Fujimoto, T. Hirakawa, S. Fukuzumi, *J. Am. Chem. Soc.* **2005**, *127*, 1216.
- [255] J. Otsuki, E. Nagamine, T. Kondo, K. Iwasaki, M. Asakawa, K. Miyake, *J. Am. Chem. Soc.* **2005**, *127*, 10400.
- [256] M. El Garah, A. Ciesielski, N. Marets, V. Bulach, M. W. Hosseini, P. Samorì, *Chem. Commun.* **2014**, *50*, 12250.
- [257] M. El Garah, N. Marets, M. Mauro, A. Aliprandi, S. Bonacchi, L. De Cola, A. Ciesielski, V. Bulach, M. W. Hosseini, P. Samorì, *J. Am. Chem. Soc.* **2015**, *137*, 8450.

- [258] L. Brinkhaus, G. Katsukis, J. Malig, R. D. Costa, M. Garcia-Iglesias, P. Vázquez, T. Torres, D. M. Guldi, *Small* **2013**, *9*, 2348.
- [259] J. Malig, A. W. I. Stephenson, P. Wagner, G. G. Wallace, D. L. Officer, D. M. Guldi, *Chem. Commun.* **2012**, *48*, 8745.
- [260] N. L. Yang, J. Zhai, D. Wang, Y. S. Chen, L. Jiang, *Acs Nano* **2010**, *4*, 887.
- [261] M. El Gemayel, S. Haar, F. Liscio, A. Schlierf, G. Melinte, S. Milita, O. Ersen, A. Ciesielski, V. Palermo, P. Samori, *Adv. Mater.* **2014**, *26*, 4814.
- [262] S. Basu, F. Adriyanto, Y. H. Wang, *Nanotechnology* **2014**, *25*.
- [263] J. Huang, D. R. Hines, B. J. Jung, M. S. Bronsgeest, A. Tunnell, V. Ballarotto, H. E. Katz, M. S. Fuhrer, E. D. Williams, J. Cumings, *Org. Electron.* **2011**, *12*, 1471.
- [264] A. Kumari, I. Singh, N. Prasad, S. K. Dixit, P. K. Rao, P. K. Bhatnagar, P. C. Mathur, C. S. Bhatia, S. Nagpal, *J. Nanophotonics* **2014**, *8*.
- [265] T. Mosciatti, S. Haar, F. Liscio, A. Ciesielski, E. Orgiu, P. Samori, *Acs Nano* **2015**, *9*, 2357.
- [266] Y. Y. Feng, H. P. Liu, W. Luo, E. Z. Liu, N. Q. Zhao, K. Yoshino, W. Feng, *Sci. Rep.* **2013**, *3*, 3260.
- [267] A. Hirsch, J. M. Englert, F. Hauke, *Accounts Chem Res* **2013**, *46*, 87.
- [268] G. L. C. Paulus, Q. H. Wang, M. S. Strano, *Accounts Chem Res* **2013**, *46*, 160.
- [269] M. Quintana, E. Vazquez, M. Prato, *Accounts Chem Res* **2013**, *46*, 138.
- [270] T. Kuila, S. Bose, A. K. Mishra, P. Khanra, N. H. Kim, J. H. Lee, *Prog. Mater. Sci.* **2012**, *57*, 1061.
- [271] R. C. Haddon, *Accounts Chem Res* **2013**, *46*, 1.
- [272] J. Park, M. D. Yan, *Accounts Chem Res* **2013**, *46*, 181.
- [273] V. Georgakilas, M. Otyepka, A. B. Bourlinos, V. Chandra, N. Kim, K. C. Kemp, P. Hobza, R. Zboril, K. S. Kim, *Chem. Rev.* **2012**, *112*, 6156.
- [274] L. Yan, Y. B. Zheng, F. Zhao, S. J. Li, X. F. Gao, B. Q. Xu, P. S. Weiss, Y. L. Zhao, *Chem. Soc. Rev.* **2012**, *41*, 97.
- [275] L. L. Jiang, Z. J. Fan, *Nanoscale* **2014**, *6*, 1922.
- [276] G. P. Liu, W. Q. Jin, N. P. Xu, *Chem. Soc. Rev.* **2015**, *44*, 5016.
- [277] L. Huang, M. Zhang, C. Li, G. Q. Shi, *J. Phys. Chem. Lett.* **2015**, *6*, 2806.
- [278] B. G. Choi, M. Yang, W. H. Hong, J. W. Choi, Y. S. Huh, *Acs Nano* **2012**, *6*, 4020.
- [279] C. M. Chen, Q. Zhang, C. H. Huang, X. C. Zhao, B. S. Zhang, Q. Q. Kong, M. Z. Wang, Y. G. Yang, R. Cai, D. S. Su, *Chem. Commun.* **2012**, *48*, 7149.
- [280] Y. W. Zhu, S. Murali, M. D. Stoller, K. J. Ganesh, W. W. Cai, P. J. Ferreira, A. Pirkle, R. M. Wallace, K. A. Cychoz, M. Thommes, D. Su, E. A. Stach, R. S. Ruoff, *Science* **2011**, *332*, 1537.
- [281] X. H. Cao, Y. M. Shi, W. H. Shi, G. Lu, X. Huang, Q. Y. Yan, Q. C. Zhang, H. Zhang, *Small* **2011**, *7*, 3163.
- [282] Y. X. Xu, Z. Y. Lin, X. Q. Huang, Y. Liu, Y. Huang, X. F. Duan, *Acs Nano* **2013**, *7*, 4042.
- [283] Y. C. Yong, X. C. Dong, M. B. Chan-Park, H. Song, P. Chen, *Acs Nano* **2012**, *6*, 2394.
- [284] X. J. Zhou, J. L. Qiao, L. Yang, J. J. Zhang, *Adv. Energy Mater.* **2014**, *4*, 1301523.
- [285] S. Goenka, V. Sant, S. Sant, *J. Control. Release* **2014**, *173*, 75.
- [286] X. Y. Li, X. L. Huang, D. P. Liu, X. Wang, S. Y. Song, L. Zhou, H. J. Zhang, *J. Phys. Chem. C* **2011**, *115*, 21567.